Plant Biotechnology Journal

WILEY | aab SEB

RESEARCH ARTICLE OPEN ACCESS

Strigolactones Regulate Sugar Allocation to Control Rice Tillering and Root Development via the *OsSPL14-OsSHR1-OsSWEET16* Pathway

Miao Feng[1] | Wenfan Luo[1] | Sheng Luo[1] | Rong Miao[2] | Manpo Gu[1] | Shuai Li[1] | Xinxin Xing[1] | Jinhui Zhang[1] | Jinsheng Qian[1] | Xin Liu[1] | Chunlei Zhou[1] | Qi Sun[1] | Tong Luo[1] | Nuo Chen[1] | Yulong Ren[1] | Zhijun Cheng[1,3] | Cailin Lei[1] | Zhichao Zhao[1] | Shanshan Zhu[1] | Xin Wang[1] | Xiuping Guo[1] | Qibing Lin[1] | Jianmin Wan[1,2,4]

[1]State Key Laboratory of Crop Gene Resources and Breeding, Institute of Crop Sciences, Chinese Academy of Agricultural Sciences, Beijing, China | [2]State Key Laboratory for Crop Genetics and Germplasm Enhancement, Nanjing Agricultural University, Nanjing, China | [3]Nanfan Research Institute, Chinese Academy of Agricultural Sciences, Sanya, China | [4]Zhongshan Biological Breeding Laboratory, Nanjing, China

Correspondence: Qibing Lin (linqibing@caas.cn) | Jianmin Wan (wanjianmin@caas.cn)

Received: 15 May 2025 | **Revised:** 17 August 2025 | **Accepted:** 8 September 2025

Funding: This work was supported by National Key Research and Development Program of China, 2022YFD1200104; Chinese Academy of Agricultural Sciences, CAAS-CSCB-202401; National Natural Science Foundation of China, 31671769.

Keywords: root development | strigolactones | sugar allocation | tillering

ABSTRACT

Strigolactones (SLs) are root-to-shoot phytohormones that regulate tillering (branching) and root development. Sugar, as an essential energy substance and signalling molecule, plays a fundamental role in the growth and development of plants. However, the molecular mechanisms by which SL directly regulates sugar allocation to control tillering and root development are still not fully understood. Here, we found that OsSHR1 operates directly downstream of OsSPL14 within the SL signalling pathway, facilitating root elongation while inhibiting tillering and crown root development. The expression of *OsSHR1* is stimulated by OsSPL3/12/14 in vivo, and D53 can interact with these SPL proteins to suppress their transcriptional activities. Interestingly, we further demonstrate that OsSHR1 can directly bind to the promoters of *OsSWEET2a/4/16*, which encode sugar transporters that can control the allocation of sugar in plant growth and development. This binding facilitates the expression of sugar transporters, which in turn regulate sugar allocation and enable the plant's response to SLs. The results indicate that via the *OsSPL14-OsSHR1-OsSWEET16* pathway, SLs orchestrate the distribution of sugars to ensure their effectiveness in stimulating root elongation while simultaneously suppressing tillering and crown root formation in rice.

1 | Introduction

Strigolactones (SLs), a class of carotenoid-derived phytohormones, act as branching-repressing hormones with highly conserved functions in both monocots and dicots (Gomez-Roldan et al. 2008; Umehara et al. 2008). In addition to repressing shoot branching, SLs also regulate root development, leaf senescence and flower development (Snowden et al. 2005; Ueda and Kusaba 2015). For example, SLs promote the elongation of primary roots and adventitious (crown) roots, and suppress crown root and lateral root formation in Arabidopsis and rice (Arite et al. 2011; Ruyter-Spira et al. 2011; Rasmussen et al. 2012; Sun et al. 2014, 2016; Kumar et al. 2015; Yuan et al. 2023).

Miao Feng, Wenfan Luo, Sheng Luo and Rong Miao contributed equally to this work.

The biosynthesis and signalling pathway of SLs has been generally elucidated. In rice, *DWARF 3* (*D3*), *DWARF14* (*D14*, *HTD2* and *D88*) and *DWARF53* (*D53*) are involved in the SL signalling (Ishikawa et al. 2005; Arite et al. 2009; Jiang et al. 2013; Zhou et al. 2013). *D14* encodes a member of the α/β-hydrolase fold family proteins, which binds and hydrolyses SLs (Arite et al. 2009; Gao et al. 2009; Yao et al. 2016; Hu et al. 2024). This triggers a conformational change of D14 to induce its binding with the F-box protein D3 to form a Skp1–Cullin–F-box (SCF) complex $SCF^{D3\text{-}D14}$ (de Saint Germain et al. 2016; Yao et al. 2016; Shabek et al. 2018). This complex then interacts with the SL signalling repressor D53, leading to its ubiquitination and subsequent degradation (Jiang et al. 2013; Zhou et al. 2013; Shabek et al. 2018). D53 degradation relieves inhibited activities of IDEAL PLANT ARCHITECTURE1 (IPA1), thereby triggering downstream SL responses that promote rice root elongation and suppress tillering (Song et al. 2017; Sun et al. 2021).

IPA1 belongs to SQUAMOSA promoter-binding-like transcription factors (SPLs), a class of plant-specific transcription factors with a highly conserved DNA-binding domain (SBP-DBD), which enables them to primarily bind DNA sequences with a GTAC core sequence (Yamasaki et al. 2004; Birkenbihl et al. 2005). Rice contains 19 SPL encoding genes, which can be categorised into six subgroups (Xie et al. 2006). Among them, eight *SPL* genes (*OsSPL3*, *OsSPL6*, *OsSPL8*, *OsSPL12*, *OsSPL13*, *OsSPL14*, *OsSPL16* and *OsSPL17*) play diverse roles in plant architecture, inflorescence architecture, leaf ligule development, panicle apical abortion, grain size, shape and quality, as well as root development (Lee et al. 2007; Jiao et al. 2010; Miura et al. 2010; Wang et al. 2012, 2018; Si et al. 2016; Shao, Zhou, et al. 2019; Sun et al. 2021). Among these *SPL* genes, *OsSPL14* (*IPA1*) can repress tillering but promote inflorescence branching in rice; and its gain-of-function mutant *ipa1-2D* with higher *IPA1* mRNA levels can promote the big panicle formation, thus increasing the rice yield (Zhang et al. 2017). *OsSPL14/17* act downstream of SL signalling to modulate rice root elongation in response to nitrate supply (Sun et al. 2021). In addition, the *OsmiR156-OsSPL3/OsSPL12* module directly activates *OsMADS50* in the node to regulate crown root development in rice. The gain-of-function mutant *lower crown root number 1* (*lcrn1*), which results from a point mutation in *OsSPL3* that disrupts the OsmiR156-mediated cleavage of *OsSPL3* transcripts, exhibited reduced crown roots and tillers (Shao, Zhou, et al. 2019).

The *Sugars Will Eventually be Exported Transporters* (*SWEET*) gene family encodes a class of sugar transporters belonging to the MtN3/saliva family with multiple transmembrane domains, which can transport sugars, sugar alcohols and hormones (Chen et al. 2010; Yuan and Wang 2013; Singh et al. 2023). As the conserved transporters of hexoses and sucrose, SWEETs play a variety of functions in plant development and production by controlling the allocation of sugars, including leaf senescence (Quirino et al. 1999), sugar loading in phloem (Chen et al. 2012), nectar production (Lin et al. 2014), pollen viability (Chu et al. 2006; Yang et al. 2006), grain filling (Sosso et al. 2015; Ma et al. 2017; Yang et al. 2018), host-pathogen interaction and various stress responses (Yang et al. 2006, 2023; Chen et al. 2010; Gao et al. 2018, 2021; Jeena et al. 2019; Breia et al. 2021; Kim et al. 2021; Mathan et al. 2021). Arabidopsis and rice genomes contain 17 and 22 *SWEET* genes, respectively and they can be grouped into four clades: clade I (*OsSWEET1a/1b/2a/2b/3a/3b*), clade II (*OsSWEET4/5/6a/6b/7a/7b/7c/7d/7e*), clade III (*OsSWEET11a/11b/12/13/14/15*) and clade IV (*OsSWEET16*) (Chen et al. 2010; Wu et al. 2022). In addition, OsSWEET3a, OsSWEET5 and OsSWEET13/15 are involved in the transport of GA_{20} to young leaves (Morii et al. 2020), the regulation of auxin signalling and auxin translocation (Zhou et al. 2014) and the response of ABA to abiotic stress (Mathan et al. 2021) in rice, respectively. A recent study has shown that *ZmCCD8* promotes the accumulation of sugars in maize kernels by upregulating the activities of *ZmSWEET10* and *ZmSWEET13c*, suggesting that SLs also regulate the expression of *SWEET* genes (Zhong et al. 2024). However, the specific mechanisms by which SWEET proteins participate in the SL signalling pathway and their precise roles in regulating plant architecture are largely unknown.

The *SHORT ROOT* (*SHR*) gene, which encodes a GRAS protein, plays a crucial role in root radial patterning and stem cell niche specification in *Arabidopsis thaliana*, in conjunction with the GRAS protein SCARECROW (SCR) (Benfey et al. 1993; Di Laurenzio et al. 1996; Helariutta et al. 2000; Nakajima et al. 2001). SHR protein is found to act as a signal from the stele to specify endodermal cell fate and activate *SCR*-mediated asymmetric cell division, thus stimulating root ground tissue (endodermis and cortex) formation to promote root meristem development in Arabidopsis (Nakajima et al. 2001). *SHR-like* genes also facilitate the development of root meristem in a variety of roots across rice, leguminous plants and maize (Henry et al. 2017; Dong et al. 2020; Lin et al. 2020; Ortiz-Ramírez et al. 2021). Besides, *SHR-like* genes regulate cell proliferation and differentiation in other organs such as the endodermis in hypocotyl and inflorescence stem (Fukaki et al. 1998) and leaf vascular, as well as bundle sheath development in Arabidopsis (Dhondt et al. 2010; Cui et al. 2014), stomatal patterns and minor vein differentiation in rice (Schuler et al. 2018; Wu et al. 2019; Liu et al. 2023), and the formation of Kranz anatomy in maize (Wang et al. 2013). As the key regulator of plant growth and development, *SHR-like* genes or the proteins they encode, are tightly regulated by multiple hormones. In Arabidopsis, abscisic acid (ABA) and gibberellin (GA) coordinate the formation of the middle cortex in the root meristem by regulating the expression of the *SHR* and *SCR* genes at the transcriptional level (Choi and Lim 2016; Gong et al. 2016; Lee et al. 2016). In rice, ABA and GA antagonistically regulate the APC/C^{TE} (an E3 ubiquitin ligase)-mediated degradation of OsSHR1 to control the OsSHR1 protein level, thereby modulating root elongation (Lin et al. 2020). However, the relationship between SLs and *SHR-like* genes remains unclear.

Here, we have demonstrated that within the SL signalling pathway, a regulatory pathway *OsSPL14-OsSHR1-OsSWEET16* alters sugar allocation in rice, effectively inhibiting tillering and crown root formation while promoting root elongation. Therefore, this study offers new insights into the specific regulatory mechanism of SL on rice plant architecture by regulating sugar allocation.

2 | Results

2.1 | *OsSHR1* Regulates Root Development and Represses Tillering in Response to SLs

We previously showed that ABA and GA antagonistically regulate APC/C^{TE}-mediated degradation of OsSHR1 to regulate root length (Lin et al. 2020). During this study, we noticed that besides the varied root lengths (Figure 1a,c), the *OsSHR1-Ri* seedlings also displayed more crown roots while the *OsSHR1-mD-His* (a stable OsSHR1 mutant with His marker) seedlings exhibited fewer crown roots than Nipponbare (Nip) seedlings (Figure 1a,b,d). Moreover, the *OsSHR1-Ri* plants displayed more tillers while the *OsSHR1-mD-His* plants showed fewer tillers compared with Nip plants (Figure 1e,f). An expression analysis of *OsSHR1* showed that *OsSHR1* is widely expressed in different tissues with higher levels in the root at the early seedling stage and higher levels in the root and leaf at the heading stage (Figure S1). Taken together, these results suggest that *OsSHR1* is a key plant architecture regulator with multiple functions in promoting root elongation, as well as inhibiting crown root formation and tillering.

Like *OsSHR1*, SLs also repress shoot branching (Gomez-Roldan et al. 2008; Umehara et al. 2008) and promote root elongation (Koltai 2011; Sun et al. 2014), suggesting a link between *OsSHR1* and the SL signalling pathway. To test this, we performed a $GR24^{5DS}$ treatment on seedlings of Nip, *OsSHR1-Ri* and *OsSHR1-mD-His* lines, *d27* and *d53* mutants, respectively. After $GR24^{5DS}$ treatment, the total root lengths of Nip, *OsSHR1-mD-His* and *d27* seedlings were significantly increased while their crown root numbers were evidently reduced (Figure 1g–i). Notably, the stimulatory effect of $GR24^{5DS}$ on the total root lengths and its inhibitory effect on crown root numbers of *OsSHR1-Ri* and *d53* seedlings were evidently attenuated (Figure 1g–i). In addition, the tiller number of *OsSHR1-Ri* plants remained largely unchanged under $GR24^{5DS}$ treatment, like that of *d53* plants (Figure 1j,k). These findings indicate that *OsSHR1* likely plays a key role within the SL signalling pathway regulating root development and tillering in rice.

2.2 | D53 Inhibits OsSPL3/12/14-Mediated Activation of *OsSHR1* Expression

To explore how *OsSHR1* is involved in the SL signalling pathway, we analysed the promoter of *OsSHR1* and found that its promoter contains six GTAC motifs (A through F) recognised by SPLs (Figure S2a) (Birkenbihl et al. 2005), suggesting that *OsSHR1* may be a direct downstream target of SPLs. Supporting this, a yeast one-hybrid (Y1H) assay showed that OsSPL3/12/14 could bind to the last GTAC motif (F motif) in the promoter of *OsSHR1* (Figure S2b), and this binding was confirmed by an electrophoretic mobility shift assay (EMSA) (Figure S2c–e). Chromatin immunoprecipitation-quantitative PCR (ChIP-qPCR) analyses showed the significant enrichment of the P2 segment containing the F motif within the *OsSHR1* promoter sequence by OsSPL3/12/14 (Figure 2a–d). Furthermore, a transient dual-LUC assay in rice protoplasts indicated that Pro35S:OsSPL3/12/14-Flag significantly enhanced the expression of the luciferase (LUC) reporter gene driven by the promoter of *OsSHR1* (Figure 2e,f). Together, these results showed that OsSPL3/12/14 proteins directly bind to the *OsSHR1* promoter to activate its expression.

Consistent with the previous report that D53 binds to OsSPL14, and together with TPL/TPR proteins represses the transcriptional activity of OsSPL14 (Song et al. 2017), we also found that besides OsSPL14, OsSPL3/12 also interact with D53 (Figure S3). Then, quantitative transactivation assays showed that the co-transfection of ProOsSHR1:LUC and Pro35S:OsSPL3/12/14-Flag more significantly up-regulated LUC activity than the co-transfection of ProOsSHR1:LUC, Pro35S:D53-GFP and Pro35S:OsSPL3/12/14-Flag (Figure 2e,f), indicating that D53 likely interacts with OsSPL3/12/14 to inhibit the transcription of *OsSHR1* promoted by them.

2.3 | OsSHR1 Positively Regulates *OsSWEET2a/4/16* Expression

Some recent studies have shown that sugars can affect the plant's response to SLs, including leaf senescence and tiller development (Tian et al. 2018; Bertheloot et al. 2019; Patil et al. 2021; Takahashi et al. 2021). As key transporters of sugars, SWEETs influence a wide range of plant development processes by regulating sugar partitioning (Chen et al. 2010, 2012; Yuan et al. 2014; Breia et al. 2021; Hu et al. 2021; Singh et al. 2023). Moreover, SLs can regulate the accumulation of sugars in grains (Zhong et al. 2024). These results suggest a connection between SLs and the distribution of sugars during plant development. In addition, the promoters of rice *SWEET* genes contain the AATTT motif that can be specifically recognised by GRAS proteins (Hirsch et al. 2009; Shi et al. 2019). Therefore, to test whether SWEETs are involved in the OsSHR1-mediated regulation of tillering and root development, we performed a Y1H assay using the promoters of 22 *OsSWEET* genes. The results indicated that OsSHR1 directly binds to the C, G, I and C sites with the AATTT motif in the promoter regions of *OsSWEET2a/4/16*, respectively (Figure S4). This finding was confirmed by an EMSA (Figure S5). ChIP-qPCR analyses with anti-GFP antibodies also verified the recruitment of OsSHR1 by the promoter regions of *OsSWEET2a/4/16* in vivo (Figure 2g–j). We further found that OsSHR1 significantly enhanced the expression of the luciferase (LUC) reporter gene driven by the promoters of *OsSWEET2a/4/16* in rice protoplasts (Figure 2k,l). These results suggest that OsSHR1 can directly bind to the promoters of *OsSWEET2a/4/16* to activate their expressions.

2.4 | *OsSHR1* Acts Downstream of *OsSPL14* to Regulate Tillering and Root Development in Response to SLs

To test the genetic relationship between *OsSHR1* and *OsSPL3/12/14*, we further generated *osspl14* single mutants, *OsSHR1-Ri/osspl14* and *OsSHR1-mD-His/osspl14* lines using the CRISPR/Cas9 genome-editing method (Figures 3a and S6a,b). Upon observation, we found that the *OsSHR1-Ri*, *osspl14* and *OsSHR1-Ri/osspl14* lines all displayed a high tillering phenotype, compared with Nip (Figure S6a,c), which makes it difficult to define the genetic relationship between *OsSHR1* and *OsSPL14*.

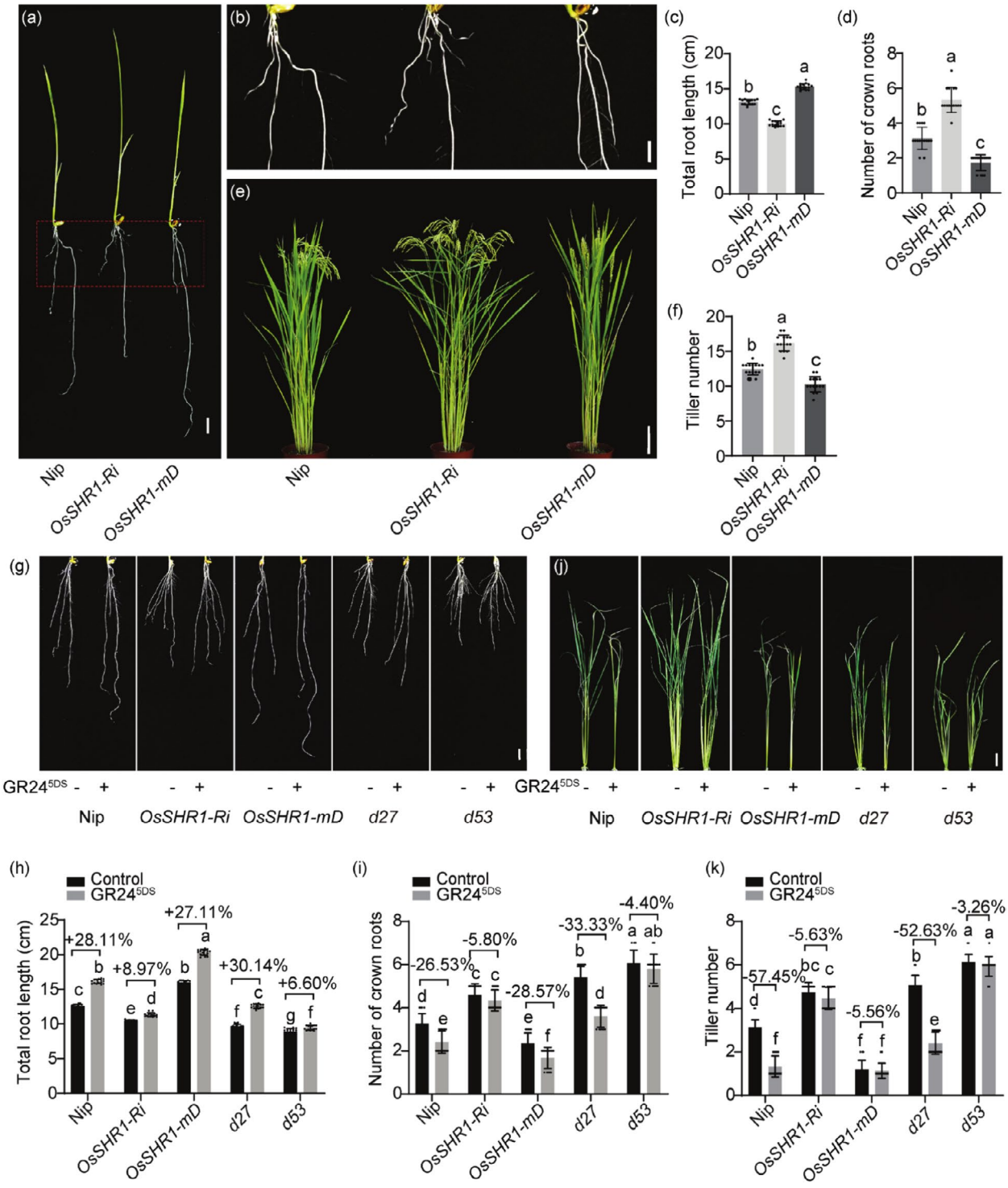

FIGURE 1 | *OsSHR1* is involved in the SL-mediated regulation of rice tiller and root development. (a) The seedling phenotype of 8-day-old Nipponbare (Nip), *OsSHR1-Ri* and *OsSHR1-mD-His*. Bar = 1 cm. (b) The crown root phenotype of the boxed area in (a). Bar = 0.5 cm. (c, d) Statistical analyses of total root length (c) and crown root number (d) in (a). Values are means ± SD. Different letters indicate significant differences ($p < 0.05$, $n = 15$, two-way ANOVA). (e) Plant morphology of Nip, *OsSHR1-Ri* and *OsSHR1-mD-His* at the mature stage. Bar = 10 cm. (f) Statistical analyses of tiller number in (e). Values are means ± SD. Different letters indicate significant differences ($p < 0.05$, $n = 15$, two-way ANOVA). (g) Root morphology of 8-day-old Nip, *OsSHR1-Ri, OsSHR1-mD-His*, *d27* and *d53* mutants with or without $GR24^{5DS}$ treatment. +, apply $GR24^{5DS}$ with 1 μM (dissolved with DMSO); −, equal volume of DMSO. Bar = 1 cm. (h, i) Statistical analyses of total root length (h) and crown root number (i) in (g). Values are means ± SD. Different letters indicate significant differences ($p < 0.05$, $n = 15$, two-way ANOVA). (j) Plant morphology of Nip, *OsSHR1-Ri*, *OsSHR1-mD-His*, *d27* and *d53* seedlings with or without $GR24^{5DS}$ treatment. +, apply $GR24^{5DS}$ with 1 μM (dissolved with DMSO); −, equal volume of DMSO. Bar = 5 cm. (k) Statistical analyses of tiller number in (j). Values are means ± SD. Different letters indicate significant differences ($p < 0.05$, $n = 15$, two-way ANOVA).

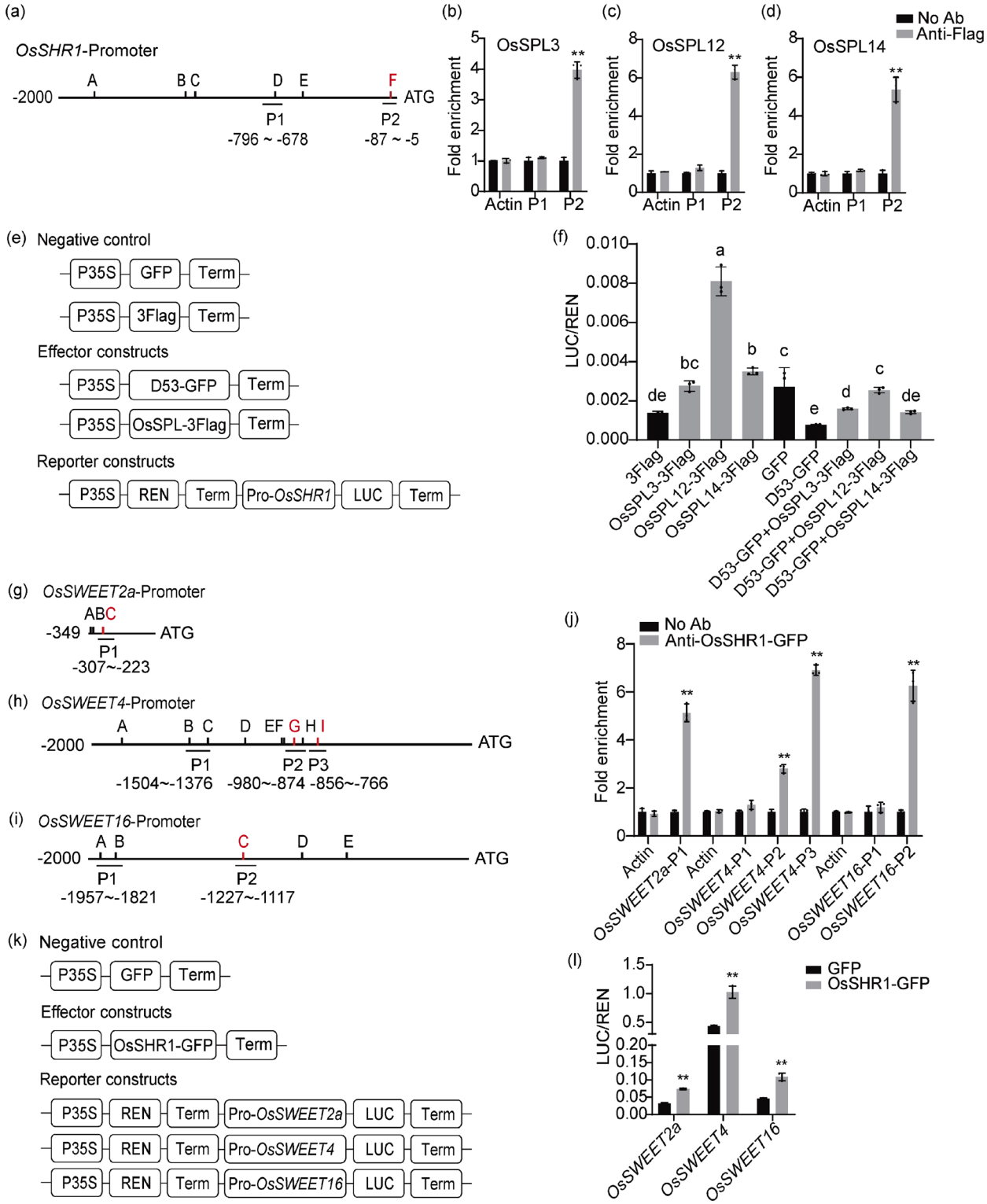

FIGURE 2 | Legend on next page.

However, the *OsSHR1-mD-His/osspl14* lines showed a median tiller number between the *OsSHR1-mD-His* line and *osspl14* single mutants, like that of Nip (Figure 3a,b), suggesting that *OsSHR1-mD-His*, a gain-of-function mutant of *OsSHR1*, could largely restore the high tillering phenotype of the *osspl14* single mutant to a normal level. To confirm this, we further constructed the *Actin1:OsSPL14*-overexpression vector and introduced it into Nip and *OsSHR1-Ri* plants to obtain *OsSPL14-OE* and *OsSHR1-Ri/OsSPL14-OE* lines (Figure S6d,e). The *OsSPL14-OE* plants showed reduced tillers while the *OsSHR1-Ri/OsSPL14-OE* plants showed a high tillering phenotype like *OsSHR1-Ri* plants, compared to Nip (Figure S6d–f). Similar genetic relationships were also observed between *OsSHR1* and *OsSPL3/12* in regulating tillering (Figures S7 and S8). These results indicate that *OsSHR1* acts downstream of *OsSPL3/12/14* to repress rice tillering.

FIGURE 2 | OsSPL3/12/14 and OsSHR1 bind to the promoters of *OsSHR1* and *OsSWEET2a/4/16*, respectively. (a) Diagram of the *OsSHR1* promoter region. The letters A to F indicate GTAC motifs. The red letter indicates the binding sites identified by EMSA. P1 and P2 represent the locations of ChIP-enriched fragments. (b–d) ChIP-qPCR analyses verify the binding of OsSPL3/12/14 to the promoter regions of *OsSHR1*. Cross-linked chromatin samples were extracted from rice protoplasts co-expressing Pro35S:OsSPL3/12/14-Flag and ProOsSHR1:Luc-Pro35S:Rluc, then were precipitated with anti-Flag antibody. No Ab (No antibody) served as negative controls. Values are means ± SD (**$p < 0.01$, $n = 3$, two-way ANOVA). (e) Effectors and reporter constructs used in the dual luciferase assay. (f) D53 represses the transcriptional activation activities of OsSPL3/12/14 on the *OsSHR1* promoter in rice protoplasts. Relative LUC activity was calculated by LUC/REN. Values are means ± SD. Different letters indicate significant differences ($p < 0.05$, $n = 3$, two-way ANOVA). (g–i) Diagrams of the *OsSWEET2a/4/16* promoter region, respectively. The letters A to I indicate AATTT motifs. The red letters indicate the binding sites identified by EMSA. P1, P2 and P3 represent the locations of ChIP-enriched fragments. (j) ChIP-qPCR analyses verify the binding of OsSHR1 to the promoter regions of *OsSWEET2a/4/16*. Cross-linked chromatin samples were extracted from rice protoplasts co-expressing Pro35S:OsSHR1-GFP and ProOsSWEET2a/4/16:Luc-Pro35S:Rluc, then were precipitated with anti-GFP antibody. No Ab (No antibody) served as negative controls. Values are means ± SD (**$p < 0.01$, $n = 3$, two-way ANOVA). (k) Effector and reporter constructs used in the dual luciferase assay. (l) OsSHR1 activates the transcriptional activity of *OsSWEET2a/4/16* in rice protoplasts. Relative LUC activity was calculated by LUC/REN. Values are means ± SD (**$p < 0.01$, $n = 3$, Student's *t*-test).

Previous studies indicated that both *SPL* and *SHR-like* genes act as key regulators of root development (Shao, Zhou, et al. 2019; Lin et al. 2020; Sun et al. 2021). To test the genetic relationships between *OsSHR1* and *OsSPL3/12/14* in root development regulation, we did additional analyses. The *OsSHR1-Ri*, *osspl14* and *OsSHR1-Ri/osspl14* lines all displayed shorter total root length and more crown roots, compared to Nip (Figure S9). However, the *OsSHR1-mD-His/osspl14* lines displayed longer total root length and fewer crown roots, a root phenotype similar to that of the *OsSHR1-mD-His* line, compared to Nip (Figure 3c–e). The *OsSPL14-OE* plants showed significantly longer total root length and fewer crown roots, while the *OsSHR1-Ri/OsSPL14-OE* plants showed shorter total root length and more crown roots like *OsSHR1-Ri* plants, compared to Nip (Figure 3f–h). Similar genetic relationships were also observed between *OsSHR1* and *OsSPL3/12* in regulating root development (Figures S10 and S11). Taken together, these results indicate that *OsSHR1* likely acts downstream of *OsSPL3/12/14* to regulate root development.

To further test whether *OsSPL14* regulates crown root formation in the SL signalling pathway, we analysed the total root length and crown root number under $GR24^{5DS}$ treatments in Nip, *osspl14* and *OsSPL14-OE* plants (Figure 3i–k). Compared with the control group, the total root lengths of Nip after $GR24^{5DS}$ treatment were significantly increased, and crown root formation was reduced, while the treatment effect on *osspl14* mutants was significantly weakened, and the treatment effect on *OsSPL14-OE* lines was not clearly different from that of Nip (Figure 3i–k). After $GR24^{5DS}$ treatment, the crown root numbers of *OsSPL14-OE* plants were not significantly reduced compared to Nip, possibly because the crown root numbers of untreated *OsSPL14-OE* plants were already at a very low level. Notably, the $GR24^{5DS}$ treatment effects on *OsSHR1-Ri* (Figure 1g–i) and *osspl14* plants (Figure 3i–k) were significantly weakened, suggesting that the regulation of SLs on rice root development is dependent on the *OsSPL14-OsSHR1* pathway.

Furthermore, immunoblot analyses showed that *OsSPL14-OE* lines accumulated more while *osspl14* mutants accumulated fewer OsSHR1 proteins compared to Nip in roots (Figure 3l). RT-qPCR analyses revealed that the expression level of *OsSHR1* was significantly increased in the *OsSPL3/12/14-OE* lines and decreased in the *osspl3/12/14* single mutants (Figures 3m and S12).

In summary, these findings support the conclusion that *OsSHR1* acts downstream of *OsSPL3/12/14* within the SL signalling pathway to promote root elongation, while inhibiting the formation of crown roots and tillers.

2.5 | *OsSHR1* Acts Upstream of *OsSWEETs* to Regulate Tillering in Response to SLs

To determine the genetic relationship of *OsSHR1* and *OsSWEETs*, a series of *ossweet16* mutants, *OsSHR1-Ri/ossweet16* and *OsSHR1-mD-His/ossweet16* lines were generated using the CRISPR/Cas9 genome-editing method (Figure 4a–c). Then we observed that both *ossweet16* mutants and *OsSHR1-Ri/ossweet16* lines displayed increased tillers, compared to Nip (Figure 4a,c,d). In contrast to the fewer tillers of the *OsSHR1-mD-His* line, *OsSHR1-mD-His/ossweet16* lines displayed more tillers, like *ossweet16* single mutants (Figure 4b,c,e). To confirm this finding, we generated the *Actin1:OsSWEET16-OE* lines (Figure 4f,g), and found that they showed reduced tiller number and plant height, a phenotype similar to that of *OsSPL14-OE* lines (Figures 4f,h and S6d,f). Together, these results indicate that *OsSWEET16* likely acts downstream of *OsSHR1* to repress tillering in rice.

To test whether *OsSWEET16* functions in the SL signalling pathway, we examined the sensitivity of the *ossweet16* mutants and *OsSWEET16-OE* lines to SL. The results showed that the high tillering phenotype of *ossweet16* mutants could not be rescued by exogenously applied $GR24^{5DS}$, in contrast to the evidently reduced tiller number of Nip by $GR24^{5DS}$ (Figure 4i,j), indicating that *ossweet16* mutants are insensitive to SL. Taken together, these results support the notion that *OsSWEET16* can repress tillering in response to SL in rice.

However, we found that although the *OsSWEET2a* overexpression lines had reduced tiller numbers compared to Nip, the *ossweet2a* mutants displayed a similar tiller number to Nip (Figure S13). In addition, the *OsSWEET4* overexpression lines also showed reduced tiller numbers compared to Nip; only the *ossweet4-2* mutant of the two mutants exhibited slightly increased tillering compared to Nip (Figure S14). These findings suggest that *OsSWEET2a/4* exert limited effects on rice tillering regulation.

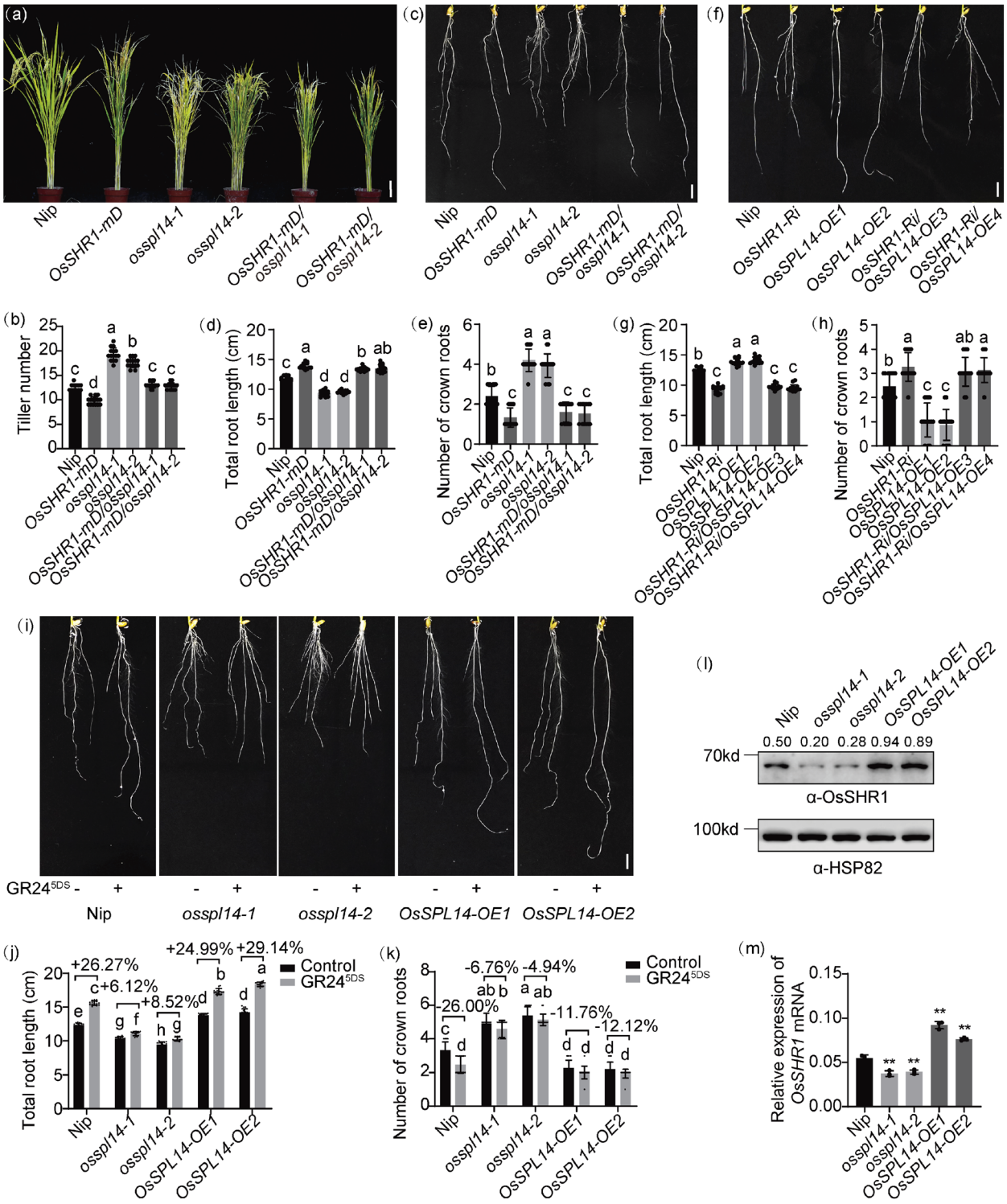

FIGURE 3 | Legend on next page.

2.6 | *OsSWEET16* Functions Downstream of *OsSPL14-OsSHR1* Pathway in the SL Signalling Pathway to Regulate Root Development

Besides more tillers, the *ossweet16* mutants also exhibited shorter total root lengths and an increased number of crown roots compared to Nip (Figure 5a–c), suggesting that *OsSWEET16* also regulates root development. The *OsSHR1-mD-His/ossweet16* lines had significantly shorter total root lengths and more crown roots, a root phenotype like that of *ossweet16* mutants (Figure 5d–f). The *Actin1:OsSWEET16-OE* lines exhibited fewer crown roots, and two of three lines exhibited slightly longer total root length compared to Nip (Figure 5g–i). Further, the root phenotypes of *ossweet2a/4* mutants showed similar results to *ossweet16* mutants, which displayed shorter total root lengths and more crown roots, and the *Actin1:OsSWEET2a-OE* lines showed longer root lengths and fewer crown roots compared with Nip (Figures S15 and

FIGURE 3 | *OsSHR1* acts downstream of *OsSPL14* in the SL signalling pathway to regulate rice tillering and root growth. (a) Plant morphology of Nip, *OsSHR1-mD-His*, *osspl14* and *OsSHR1-mD-His/osspl14* plants at the mature stage. Bar = 10 cm. (b) Statistical analyses of tiller number in (a). Values are means ± SD. Different letters indicate significant differences ($p < 0.05$, $n = 15$, two-way ANOVA). (c) Root morphology of 7-day-old Nip, *OsSHR1-mD-His*, *osspl14* and *OsSHR1-mD-His/osspl14* plants. Bar = 1 cm. (d, e) Statistical analyses of total root length (d) and crown root number (e) in (c). Values are means ± SD. Different letters indicate significant differences ($p < 0.05$, $n = 15$, two-way ANOVA). (f) Root morphology of 7-day-old Nip, *OsSHR1-Ri*, *OsSPL14-OE* and *OsSHR1-Ri/OsSPL14-OE* plants. Bar = 1 cm. (g, h) Statistical analyses of total root length (g) and crown root number (h) in (f). Values are means ± SD. Different letters indicate significant differences ($p < 0.05$, $n = 15$, two-way ANOVA). (i) Root morphology of 8-day-old Nip, *osspl14* and *OsSPL14-OE* seedlings with or without $GR24^{5DS}$ treatment. +, apply $GR24^{5DS}$ with 1 μM (dissolved with DMSO); −, equal volume of DMSO. Bar = 1 cm. (j, k) Statistical analyses of total root length (j) and crown root number (k) in (i). Values are means ± SD. Different letters indicate significant differences ($p < 0.05$, $n = 15$, two-way ANOVA). (l) Immunoblot analyses show the levels of OsSHR1 protein in the root of Nip, *osspl14* and *OsSPL14-OE* plants. 'α-HSP82' antibody was used as the loading control. The numbers above the bands indicate the relative ratio of OsSHR1/HSP82. (m) Relative expression of *OsSHR1* in Nip, *osspl14* and *OsSPL14-OE* roots. Values are means ± SD (**$p < 0.01$, $n = 3$, two-way ANOVA).

S16). These results indicate that all *OsSWEET2a/4/16* participate in regulating rice root elongation and crown root formation.

To verify whether *OsSWEET16* is also involved in the SL signalling pathway to regulate root development, we further treated *ossweet16* mutants and *OsSWEET16-OE* lines with $GR24^{5DS}$. The $GR24^{5DS}$ treatment effects on root elongation and crown root formation in *ossweet16* mutants were significantly diminished, and the treatment's impact on the root elongation of *OsSWEET16-OE* lines did not markedly differ from the impact on Nip (Figure 5j–l), suggesting that *ossweet16* mutants are insensitive to SLs.

Further, RT-qPCR analyses showed that the expression levels of *OsSWEET16* were increased in the *OsSHR1-mD-His* and *OsSPL3/12/14-OE* plants but decreased in the *OsSHR1-Ri* and *osspl3/12/14* plants (Figures 5m and S17). In line with this, the *OsSHR1-mD-His* and *OsSPL14-OE* plants accumulated more, while the *OsSHR1-Ri* and *osspl14* plants accumulated fewer OsSWEET16 proteins in their seedling roots compared to Nip (Figure 5n,o). Furthermore, the expression levels of *OsSWEET2a/4* were also decreased in the *OsSHR1-Ri* and *osspl14* plants but increased in the *OsSHR1-mD-His* and *OsSPL14-OE* plants (Figure S18).

In all, these results confirm that *OsSWEET2a/4/16* acts downstream of the *OsSPL14-OsSHR1* pathway in the SL signalling pathway to regulate root development.

2.7 | SL Regulates Sugar Allocation to Control Root Growth and Tillering via the *OsSPL14-OsSHR1-OsSWEET16* Pathway

As shown above, *OsSWEET16* acts downstream of the *OsSPL14–OsSHR1* pathway of SL signalling (Figures 4 and 5), so we speculated that SLs likely regulate the expression of *OsSWEET2a/4/16* to alter sugar distribution to affect tillering and root development in rice. As expected, the *d53* mutant accumulated fewer OsSHR1 and OsSWEET16 proteins than its wild type Norin8 (Figure 6a); the transcription levels of *OsSPL3/12/14*, *OsSHR1* and *OsSWEET2a/4/16*, and the protein levels of OsSHR1 and OsSWEET16 were induced by the $GR24^{5DS}$ treatment in Nip roots (Figure 6b,c).

To verify the function of OsSWEET2a/4/16 as sugar transporters, we explored their subcellular localization in rice protoplasts and sugar transport activity in yeast cells. Subcellular localization analyses showed that both OsSWEET2a and OsSWEET4 are located at the plasma membrane and tonoplast, while OsSWEET16 is only expressed at the tonoplast (Figure S19). The heterologous expression of OsSWEET2a enabled the growth of EBY.VW4000, a hexose transport-deficient yeast strain, on the medium supplemented with fructose, while its growth on the medium supplemented with glucose was relatively slow; and the expression of OsSWEET4/16 enabled the growth of EBY.VW4000 on the medium supplemented with glucose and fructose (Figure 6d). In addition, compared with the corresponding cells transformed with the control empty vector, the sucrose uptake-deficient strain SUSY7/ura3 cells transformed with pDR196 containing OsSWEET4/16 showed faster growth on the medium with sucrose as the sole carbon source, whereas the SUSY7/ura3 yeast cells transformed with OsSWEET2a grew more slowly (Figure 6e). These results indicate that OsSWEET2a/4/16 all have the ability to transport sugars in vivo: OsSWEET2a has a relatively strong ability to transport fructose, while OsSWEET4/16 can transport glucose, fructose and sucrose.

Sucrose is enzymatically hydrolyzed into glucose and fructose for respiration to maintain plant growth at night (Schleucher et al. 1998). To verify whether *OsSWEET2a/4/16* has rhythmic expression patterns, we performed the RT-qPCR and found that *OsSWEET2a/4/16* exhibits circadian changes at the mRNA level in tiller buds and the roots of 6-week-old Nip seedlings. Under light, the gene expression levels of *OsSWEET2a/4/16* gradually decreased, while in the dark, their expression levels showed a gradually increasing trend. Additionally, in the Nip seedlings treated with $GR24^{5DS}$, the expression levels of *OsSWEET2a/4/16* in tiller buds and roots all showed an upward trend (Figure S20).

Next, to verify whether *OsSWEET2a/4/16* affects sugar distribution in rice root and tiller buds. Given the higher expression levels of *OsSWEET2a/4/16* at the end of dark, we measured the soluble sugar levels in Nip, *OsSHR1-Ri* and *ossweet2a/4/16* mutants with or without $GR24^{5DS}$ treatment at the end of dark. Results showed that compared with Nip, the *OsSHR1-Ri* accumulated more fructose, glucose and sucrose in tiller buds and more fructose and sucrose in roots; and *ossweet2a/4/16* mutants accumulated more fructose, glucose and sucrose in both tiller

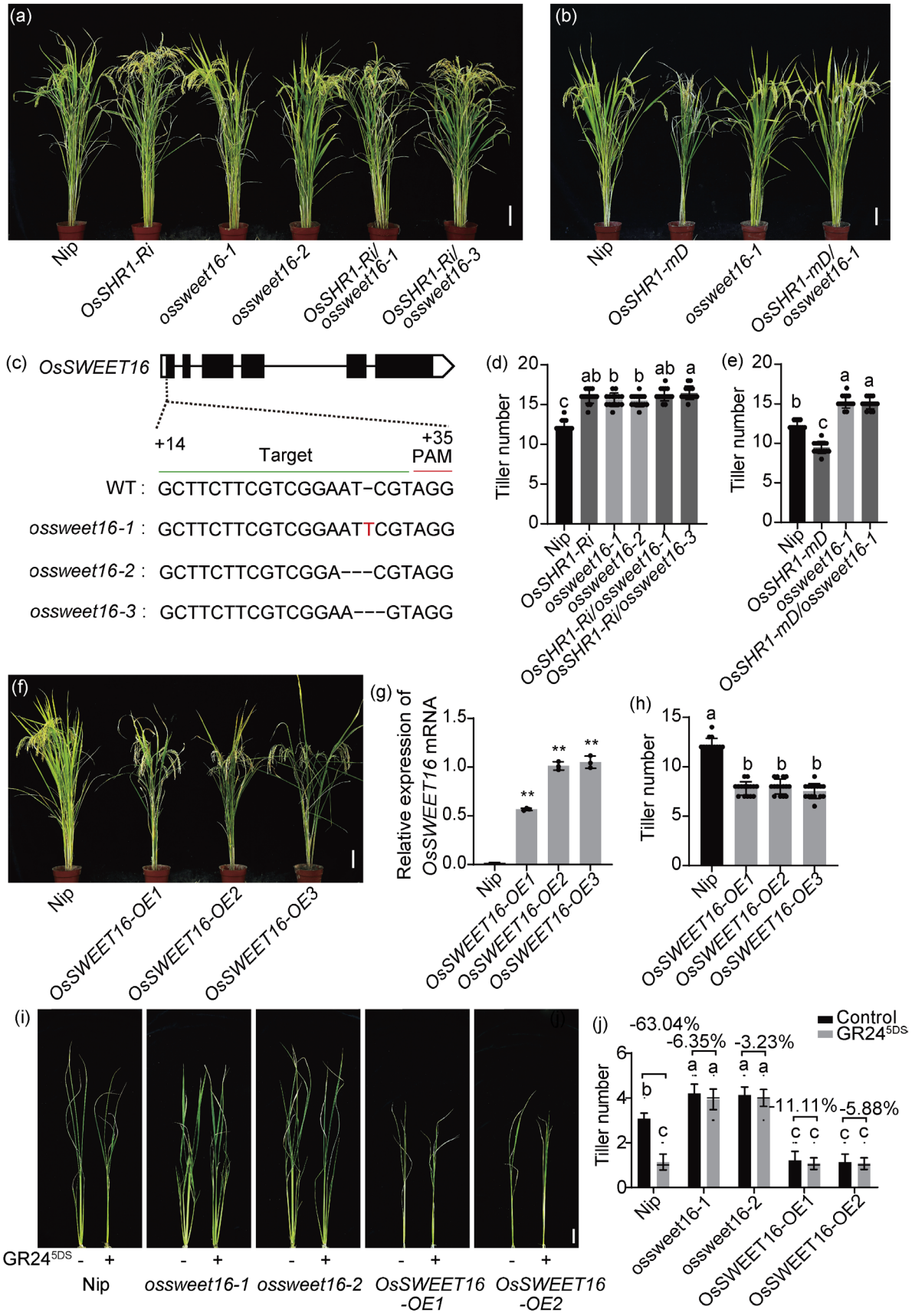

FIGURE 4 | Legend on next page.

FIGURE 4 | *OsSHR1* acts upstream of *OsSWEET16* in the SL signalling pathway to regulate rice tillering. (a, b) Plant morphology of Nip, *OsSHR1-Ri*, *ossweet16*, *OsSHR1-Ri/ossweet16*, *OsSHR1-mD-His* and *OsSHR1-mD-His/ossweet16* plants at the mature stage. Bar = 10 cm. (c) Generation and sequence analyses of *ossweet16*, *OsSHR1-Ri/ossweet16* and *OsSHR1-mD-His/ossweet16* lines produced using a CRISPR/Cas9 genome-editing approach. The guide RNA targeting sites and PAMs are indicated. A black dash indicates the deletion of one base pair. Red letters represent inserted bases. (d, e) Statistical analyses of tiller number in (a) and (b), respectively. Values are means ± SD. Different letters indicate significant differences ($p < 0.05$, $n = 15$, two-way ANOVA). (f) Plant morphology of Nip and *OsSWEET16-OE* plants at the mature stage. Bar = 10 cm. (g) Relative expression of *OsSWEET16* in Nip and *OsSWEET16-OE* plants. Values are means ± SD (**$p < 0.01$, $n = 3$, two-way ANOVA). (h) Statistical analyses of tiller number in (f). Values are means ± SD. Different letters indicate significant differences ($p < 0.05$, $n = 15$, two-way ANOVA). (i) Plant morphology of Nip, *ossweet16* and *OsSWEET16-OE* seedlings with or without $GR24^{5DS}$ treatment. Seedlings were treated with 1.0 μM $GR24^{5DS}$ (+) or mock (−). Bar = 5 cm. (j) Statistical analyses of tiller number in (i). Values are means ± SD. Different letters indicate significant differences ($p < 0.05$, $n = 15$, two-way ANOVA).

buds and roots (Figure 6f,g). Further, fructose, glucose and sucrose treatment all promoted the growth of rice tiller buds to varying degrees (Figure S21), and treatments with 0.5% to 2% fructose, glucose and sucrose all significantly inhibited the elongation of rice roots, while treatments with fructose and sucrose promoted the formation of crown roots (Figure S22). These findings indicate that the accumulation of sugars in the tiller buds and roots of *OsSHR1-Ri* and *ossweet2a/4/16* mutants likely results in their shorter roots and more crown roots and tillers. Notably, only the accumulation of fructose and glucose in tiller buds, as well as the accumulation of fructose and sucrose in roots were repressed by $GR24^{5DS}$ treatment in Nip when compared with the control group, and *OsSHR1-Ri* and *ossweet2a/4/16* mutants did not exhibit significant changes in the sugar contents in tiller buds and roots after $GR24^{5DS}$ treatment (Figure 6f,g). Based on the colour changes: the stained colours of amylose and amylopectin shift from a vivid reddish-brown to a rich blue-black as starch concentration increases (Figure S23), we found that $GR24^{5DS}$ treatment reduced starch accumulation in Nip root tips and the regions at the stem base where crown roots and tiller buds develop, and the *OsSHR1-Ri* and *ossweet16* plants exhibited significant starch accumulation in these regions, which were unaffected by $GR24^{5DS}$ (Figure 7a,b). These results suggest that the regulation of different sugar contents in rice plants by the SL signalling depends on the functions of OsSWEET proteins to varying degrees.

In addition, RNA in situ hybridization revealed that both *OsSHR1* and *OsSWEET16* were evidently expressed throughout the root meristem zone of crown root primordium, as well as in the tiller buds (Figure 7c,d), which is consistent with their roles in regulating root growth and tillering.

In summary, these results support the notion that the *OsSPL14-OsSHR1-OsSWEET16* pathway in the SL signalling pathway can alter sugar distribution in vivo to regulate tillering and root development in rice.

3 | Discussion

Many studies have shown that SLs promote the elongation of primary and crown roots while suppressing the formation of crown and lateral roots in rice and Arabidopsis (Arite et al. 2011; Kapulnik et al. 2011; Ruyter-Spira et al. 2011; Rasmussen et al. 2012; Kumar et al. 2015; Yuan et al. 2023). Notably, as a key hormone in response to low soil nutrients, SLs are induced by low soil nutrient conditions such as low phosphorus and low nitrogen conditions, to promote root elongation and inhibit lateral roots to absorb more soil nutrients in deeper soil (Sun et al. 2014; Yuan et al. 2023). Further investigation revealed that SLs suppress the density of lateral roots by downregulating the expression of *CROWN ROOTLESS 1* (*CRL1*), a key gene that facilitates the development of crown roots and lateral roots (Inukai et al. 2005; Yuan et al. 2023). In addition, as the key SL signalling genes, some *SPL* genes including *OsSPL14* can significantly promote root elongation and repress tillering (Jiao et al. 2010; Kerr and Beveridge 2017; Song et al. 2017; Sun et al. 2021). Although IPA1 (OsSPL14) can directly promote the expression of *OsTB1* to repress tillering (Lu et al. 2013), whether there is a direct downstream regulatory pathway regulated by these *SPL* genes to promote root elongation remains unclear.

Here, we report that within the SL signalling pathway, SPLs and D53 directly regulate the expression of *OsSHR1* to promote root elongation and inhibit crown root formation and tillering (Figures 1 and 2a–f; Figures S2 and S3). Our previous research revealed that *OsSHR1* promotes root development in rice by sustaining the activity and size of the root meristem (Lin et al. 2020). This study further showed that *OsSHR1* was also induced by SL (Figure 6a–c), acting as a positive regulator of SL signalling to promote root elongation and inhibit tillering and crown root formation in rice (Figure 1). Notably, the repressive effect of *OsSHR1* on tillering is different from the promoting effects of other GRAS genes such as *MONOCULM1 (MOC1)*, *DWARF AND LOW-TILLERING* (*DLT*) and *SLENDER RICE1* (*SLR1*) (Li et al. 2003; Tong et al. 2009, 2012; Liao et al. 2019; Shao, Lu, et al. 2019), indicating that the *SHR* clade of the GRAS gene family plays a distinct role in regulating rice tillering, differing from other clades, offering novel insights into the functional diversification of the GRAS gene family.

At present, it is known that *OsSWEET2a* (clade I) and *OsSWEET4* (clade II) respectively regulate sheath blight (ShB) resistance and grain filling (Sosso et al. 2015; Gao et al. 2021; Yang et al. 2023), and there is no report on the function of *OsSWEET16* yet. Here, we found that three *SWEET* genes, *OsSWEET2a/4/16*, are all involved in regulating root elongation, crown root formation and tillering to varying degrees (Figures 4 and 5; Figures S13–S16). Further, we found that SLs modulate the sugar distribution to shape plant architecture by regulating the expression of *SWEET* genes in rice (Figures 4–6; Figures S13–S16). Notably, *OsSWEET16* belongs to clade IV, along with *AtSWEET16* and *AtSWEET17* from

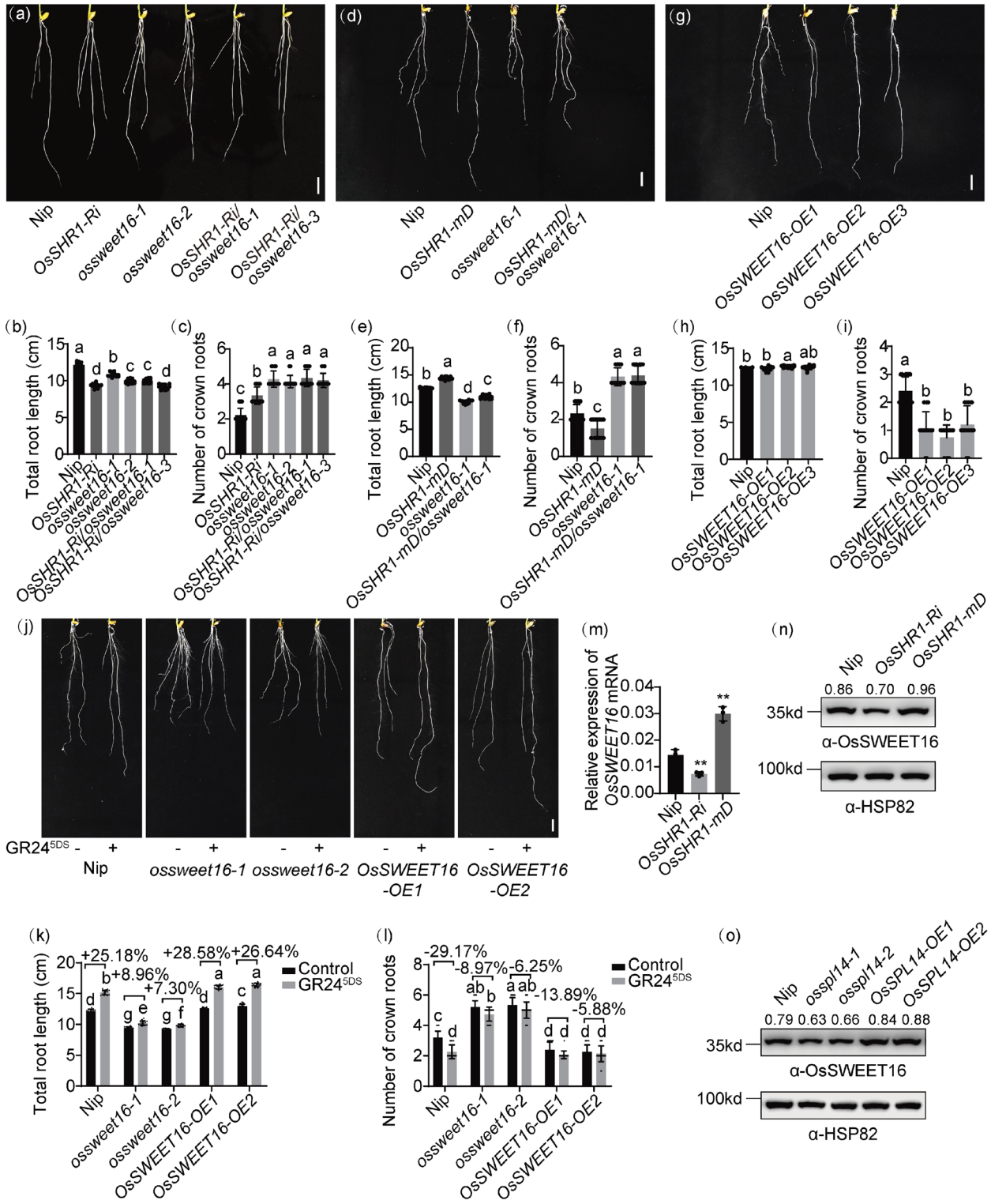

FIGURE 5 | Legend on next page.

Arabidopsis thaliana (Chen et al. 2010), and all of them are located at the tonoplast, serving as fructose, glucose and sucrose transporters (Figures 6d,e and S19c) (Chardon et al. 2013; Klemens et al. 2013; Guo et al. 2014; Valifard et al. 2021). AtSWEET17 can promote primary root elongation and reduce the fructose-mediated inhibition on the primary root elongation in *Arabidopsis thaliana* (Valifard et al. 2021). Besides, AtSWEET16 regulates germination, growth and stress tolerance in Arabidopsis, and transports out glucose, fructose and sucrose from the leaves at the end of the night (Klemens et al. 2013). Consistent with these findings, the *ossweet16* mutants also display shorter roots and more tillers, alongside striking accumulation of fructose and glucose in the tiller buds and roots, while sucrose accumulation was less pronounced (Figures 4, 5 and 6f,g). Therefore, the members of the SWEET family in clade IV may conservatively play an important role

FIGURE 5 | *OsSHR1* acts upstream of *OsSWEET16* in the SL signalling pathway to regulate root growth. (a) Root morphology of 7-day-old Nip, *OsSHR1-Ri*, *ossweet16* and *OsSHR1-Ri/ossweet16* plants. Bar = 1 cm. (b, c) Statistical analyses of total root length (b) and crown root number (c) in (a). Values are means ± SD. Different letters indicate significant differences ($p < 0.05$, $n = 15$, two-way ANOVA). (d) Root morphology of 7-day-old Nip, *OsSHR1-mD-His*, *ossweet16* and *OsSHR1-mD-His/ossweet16* plants. Bar = 1 cm. (e, f) Statistical analyses of total root length (e) and crown root number (f) in (d). Values are means ± SD. Different letters indicate significant differences ($p < 0.05$, $n = 15$, two-way ANOVA). (g) Root morphology of 7-day-old Nip and *OsSWEET16-OE* plants. Bar = 1 cm. (h, i) Statistical analyses of total root length (h) and crown root number (i) in (g). Values are means ± SD. Different letters indicate significant differences ($p < 0.05$, $n = 15$, two-way ANOVA). (j) Root morphology of 8-day-old Nip, *ossweet16* and *OsSWEET16-OE* seedlings with (+) or without (−) 1.0 μM $GR24^{5DS}$ treatment. Bar = 1 cm. (k, l) Statistical analyses of total root length (k) and crown root number (l) in (j). Values are means ± SD. Different letters indicate significant differences ($p < 0.05$, $n = 15$, two-way ANOVA). (m) Relative expression of *OsSWEET16* in Nip, *OsSHR1-Ri* and *OsSHR1-mD-His* roots. Values are means ± SD (**$p < 0.01$, $n = 3$, two-way ANOVA). (n, o) Immunoblot analyses show the levels of OsSWEET16 protein in the root of Nip, *OsSHR1* and *OsSPL14* mutants. 'α-HSP82' antibody was used as the loading control. The numbers above the bands indicate the relative ratio of OsSWEET16/HSP82.

in the transport of fructose, glucose and sucrose during plant development. Besides, there may be functional redundancy and/or diversification among OsSWEET2a, OsSWEET4 and OsSWEET16 proteins. Consistent with this hypothesis, we observed that *OsSWEET2a/4/16* exhibited different expression patterns, among which *OsSWEET2a/16* showed high expression in rice seedlings and seedling roots, while *OsSWEET4* displayed high expression in young panicles at the heading stage (Figure S24). Additionally, OsSWEET2a/4/16 showed distinct subcellular localization patterns (Figure S19). Among them, OsSWEET4 and OsSWEET16 seem to play a more crucial role in the sugar transport of tiller buds, and the mutants show a more significant accumulation of fructose and glucose (Figure 6f,g), which may be the reason why the tiller phenotypes of the *ossweet4/16* mutants are more pronounced than those of *ossweet2a* (Figure 4a–e; Figures S13 and S14).

Recent studies have revealed that sugars play key roles in regulating plant growth and development by affecting the SL signalling pathway. Sugars appear to be consistent with the SL pathway in promoting grain development. In *ZmCCD8* overexpression lines, enhanced *ZmCCD8* transcription promotes SL biosynthesis, upregulates the expression of *ZmSWEET10*, *ZmSWEET13c* and *ZmLHT14*, leading to enhanced accumulation of sugar and amino acids in maize kernels (Zhong et al. 2024). However, in leaves and tillers, sugars negatively regulate plant responses to SL. For instance, glucose reduces SL-induced leaf senescence in rice and bamboo (Tian et al. 2018; Takahashi et al. 2021), and sucrose alleviates SL-mediated inhibition of axillary bud outgrowth in rose and pea (Bertheloot et al. 2019). In rice seedlings, sucrose inhibits the degradation of the repressor protein D53 of SL signalling to alleviate the SL-induced inhibition of tiller bud outgrowth (Patil et al. 2021). Similarly, we found that the mutation of *OsSWEET16* also causes sugar accumulation in tiller buds and roots (Figure 6f,g), and renders insensitivity to SLs, thus promoting the formation of tillers and crown roots (Figures 4i,j and 5j–l). Conversely, our study also showed that SL can orchestrate sugar allocation to effectively regulate root growth and tillering, thus discovering a complex crosstalk between sugar and SL.

In all, we discovered an important regulatory pathway comprising OsSPLs, OsSHR1 and OsSWEETs that works directly downstream of *OsSPL14* within the SL signalling pathway to regulate root development and tillering (Figure 7e). In the absence of SLs, D53 binds to OsSPL14 and together with TPL/TPR proteins represses the transcriptional activation of OsSPL14 on downstream genes such as *OsTB1* and *OsSHR1* and its feedback on *D53* transcription. Repressed *OsSHR1* expression thus inhibits the transcription of *OsSWEET16*, leading to the fructose and glucose accumulation in tiller buds, fructose and sucrose accumulation in roots, finally resulting in increased tillers and crown roots and reduced root length. In response to SLs, D53 is degraded by the proteasome system, thus releasing OsSPL14 to induce transcription of *D53* and *OsTB1*, thereby inhibiting rice tiller development. Simultaneously, OsSPL14 also activates the expression of *OsSHR1*; the expressed OsSHR1 further promotes the transcription of *OsSWEET16*, thus reducing the glucose and fructose accumulation in tiller buds, fructose and sucrose accumulation in roots, finally resulting in reduced tillers and crown roots but an increased root length. Thus, our study enhances the comprehension of the regulatory mechanisms by which SLs oppositely affect rice root elongation and the formation of crown roots and tillers, offering a novel regulatory pathway to balance the rice root system and tiller number for improving rice yield.

4 | Experimental Procedures

4.1 | Plant Materials and Growth Conditions

The RNA interference (RNAi) transgenic lines of *OsSHR1* and transgenic plants expressing the undegradable OsSHR1-mD-His protein (driven by its endogenous promoter) in the Nip background used in this study were previously described (Lin et al. 2020).

Rice plants were cultivated in paddy fields during the normal growing seasons in Beijing (40°13′ N, 116°13′ E). Hydroponically cultured rice seedlings were grown in the climate chamber (HP1500GS; Ruihua) at 70% humidity, under short-day conditions with daily cycles of 10 h of light at 30°C and 14 h of dark at 25°C. Light was provided by white-light emitting diode tubes (400–700 nm, 250 μmol $m^{-2} s^{-1}$).

4.2 | Plasmid Construction and Transformation

For knocking out *OsSPL3/12/14* and *OsSWEET2a/4/16*, 19-bp gene-specific sequences targeting the exons were inserted into the sgRNA/Cas9 vector (Biogle, BGK01-G418) to generate the *OsSPL3/12/14*-Cas9 and *OsSWEET2a/4/16*-Cas9 constructs.

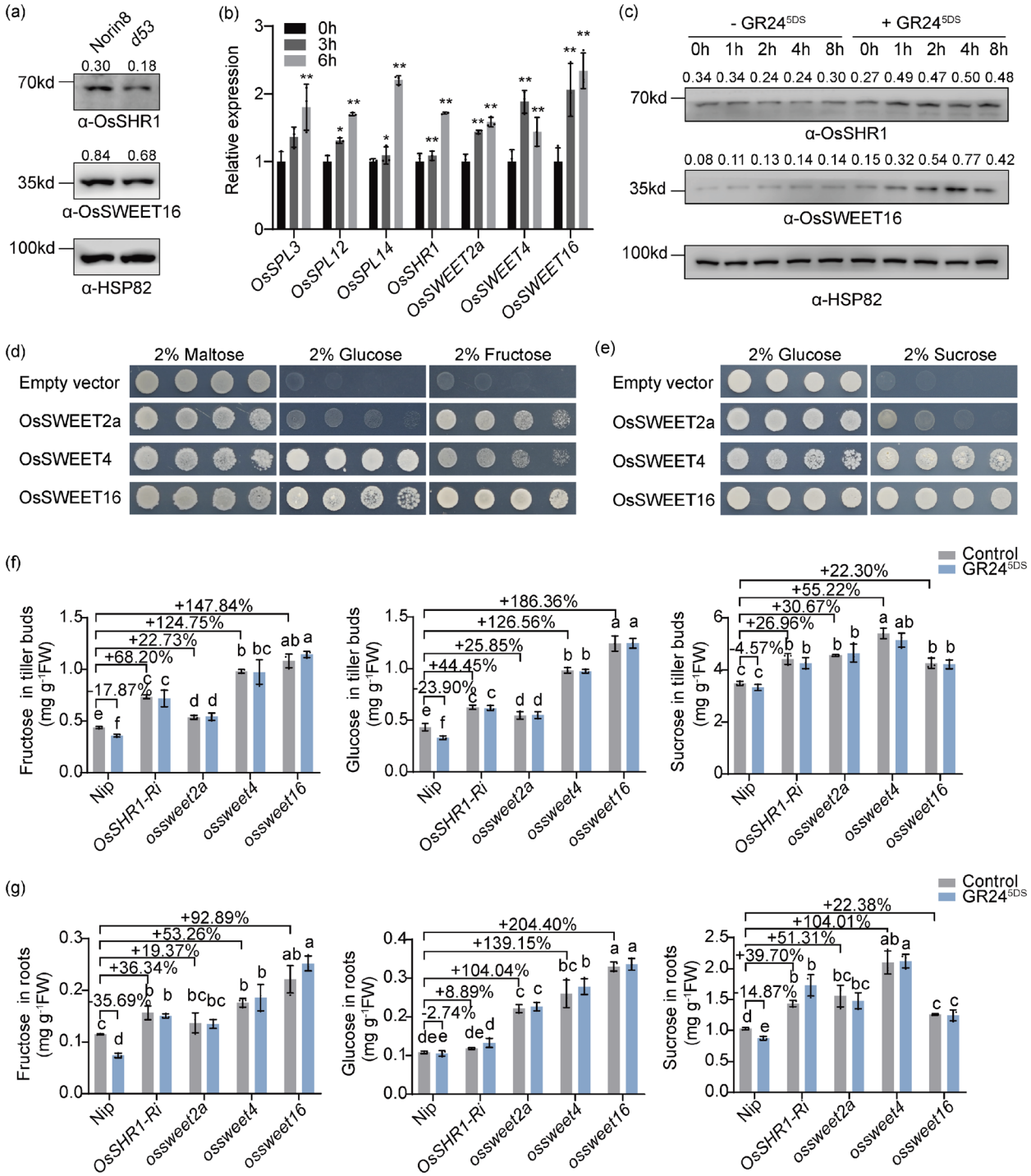

FIGURE 6 | SLs modulate sugar allocation in rice by activating the expression of *OsSWEETs*. (a) Immunoblot analysis shows the levels of OsSHR1 and OsSWEET16 proteins in the roots of 7-day-old Norin8 and *d53* plants. 'α-HSP82' antibody was used as the loading control. The numbers above the bands indicate the relative ratio of OsSHR1/HSP82 or OsSWEET16/HSP82. (b) Relative expressions of *OsSPL3/12/14*, *OsSHR1* and *OsSWEET2a/4/16* in the roots of 7-day-old Nip plants with GR24^{5DS} treatment for 6 h. The gene expression levels before treatment with GR24^{5DS} were set as '1'. Values are means ± SD (**$p < 0.01$, *$p < 0.05$, $n = 3$, two-way ANOVA). (c) Immunoblot analysis shows the levels of OsSHR1 and OsSWEET16 proteins in the roots of 7-day-old Nip plants with or without GR24^{5DS} treatment for 8 h. 'α-HSP82' antibody was used as the loading control. The numbers above the bands indicate the relative ratio of OsSHR1/HSP82 or OsSWEET16/HSP82. (d) The transport activity analysis of OsSWEET2a/4/16 in yeast cells. Growth of the yeast mutant strain EBY.VW4000 expressing different genes in SD (-Ura) media supplemented with different carbon sources (2% maltose, 2% glucose or 2% fructose). Yeast mutant strains transformed with the pDR196 empty vector were used as negative control. (e) Growth of the yeast mutant strain SUSY7/ura3 expressing different genes in SD (-Ura) media supplemented with 2% glucose or 2% sucrose. Yeast mutant strains transformed with the pDR196 empty vector were used as negative control. (f, g) The concentrations of soluble sugars (fructose, glucose and sucrose) in the tiller buds and roots of 6-week-old Nip, *OsSHR1-Ri* and *ossweet2a/4/16* mutants with or without GR24^{5DS} treatment. The samples were collected at the end of the dark. Different letters indicate significant differences ($p < 0.05$, $n = 3$, one-way ANOVA).

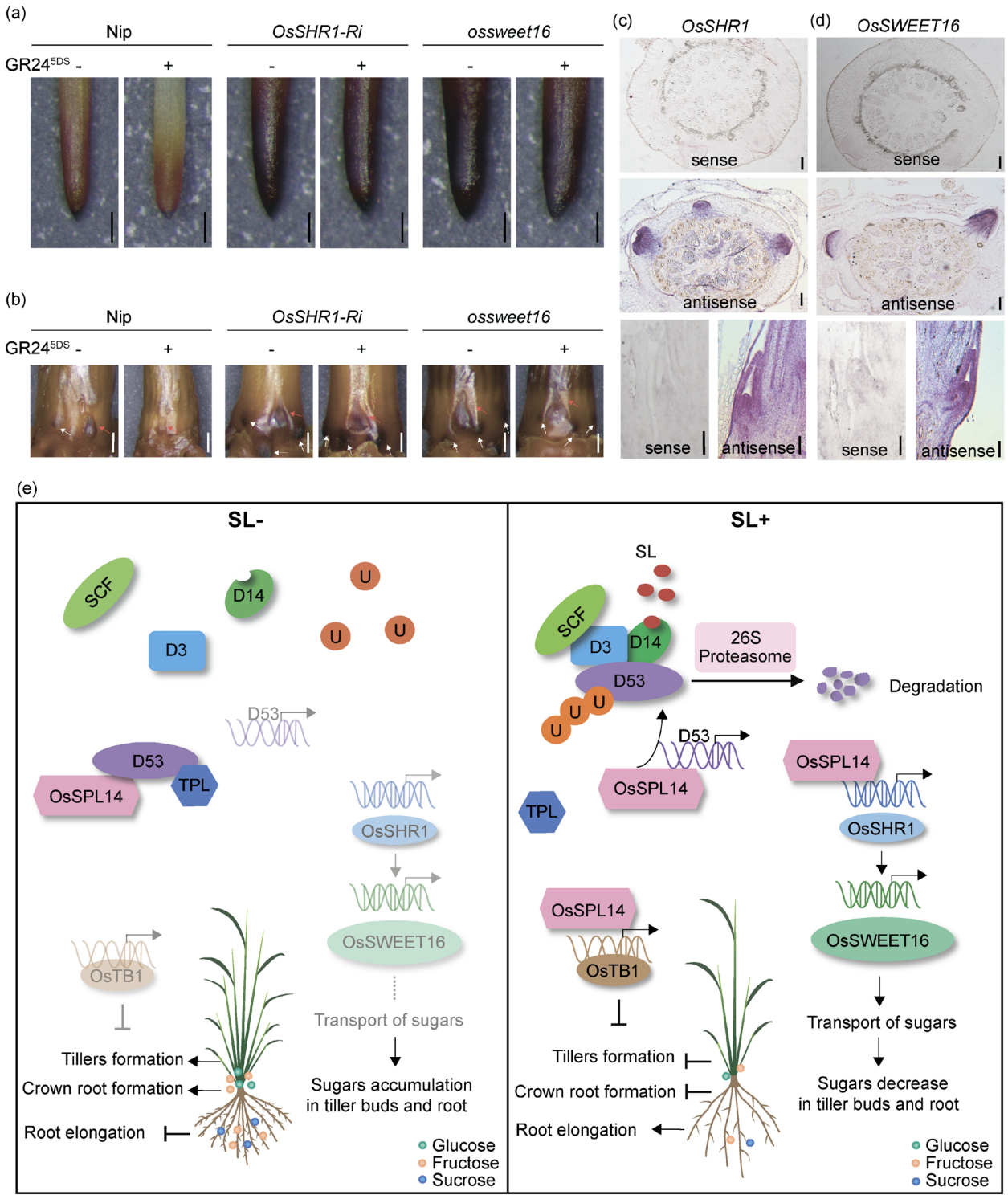

FIGURE 7 | Legend on next page.

Then the constructs were introduced into the calli of Nip, *OsSHR1-Ri* and *OsSHR1-mD-His* via Agrobacterium-mediated transformation. T0 transgenic lines were analysed by sequencing. T2 homozygous transgenic lines of each knockout line were selected and used for phenotypic observation.

For the *OsSPL3/12/14* and *OsSWEET2a/4/16* overexpression constructs, the full-length coding sequences were amplified and ligated to the pCAMBIA2300 vector (at the SmaI site) to generate the overexpression constructs. Then the constructs were introduced into Nip or *OsSHR1-Ri* calli via Agrobacterium-mediated transformation. All transgenic lines were analysed with stable T2 to T3 progeny. All primers used in this assay are listed in Table S1.

4.3 | RNA Extraction and RT-qPCR Analysis

Total RNA of different tissues or genotypes was extracted using the ZR Plant RNA MiniPrep Kit (Zymo Research, R2024)

FIGURE 7 | *OsSPL14-OsSHR1-OsSWEET16* regulatory pathway regulates root development and tillering by modulating sugar allocation in response to SLs. (a) Iodine staining of temporary starch accumulation in the primary root tip of the Nip, *OsSHR1-Ri* and *ossweet16* 7-day-old plants with or without $GR24^{5DS}$ treatment. Bar = 100 μm. (b) Iodine staining of temporary starch accumulation in the stem base of the Nip, *OsSHR1-Ri* and *ossweet16* 4-week-old plants with or without $GR24^{5DS}$ treatment. The red arrow indicates the tiller bud, the white arrow indicates the emerging crown root. Bar = 500 μm. (c, d) RNA in situ hybridization of *OsSHR1* and *OsSWEET16* in crown root primordia and tiller buds. The sense probes were used as negative controls. Bar = 100 μm. (e) A proposed working model for the regulation of rice tillering and root development by the *OsSPL14-OsSHR1-OsSWEET16* pathway in SL signalling. In the absence of SLs, D53 binds to OsSPL14 and together with TPL/TPR proteins represses the transcriptional activation of OsSPL14 on downstream genes such as *OsTB1* and *OsSHR1* and its feedback on *D53* transcription. Repressed *OsSHR1* expression thus inhibits the transcription of *OsSWEET16*, leading to the fructose and glucose accumulation in tiller buds, fructose and sucrose accumulation in roots, finally resulting in increased tillers and crown roots and reduced root length. In response to SLs, D53 is degraded by the proteasome system, thus releasing OsSPL14 to induce transcription of *D53* and *OsTB1*, thereby inhibiting rice tiller development. Simultaneously, OsSPL14 also activates the expression of *OsSHR1*; the expressed OsSHR1 further promotes the transcription of *OsSWEET16*, thus reducing the glucose and fructose accumulation in tiller buds, fructose and sucrose accumulation in roots, finally resulting in reduced tillers and crown roots but an increased root length.

following the manufacturer's recommendations. Then mRNAs were reverse transcribed using a Reverse Transcription Kit (Qiagen, 205311). RT-qPCR analyses were performed on the CFX96 Real-Time System (BIO-RAD) with the SYBR Premix Ex Taq Kit (TaKaRa, RR820). The rice *Ubiquitin* (*UBQ*) gene was used as an internal control. Primer pairs used for RT-qPCR analysis are listed in Table S2.

4.4 | Y1H Assay

Full-length coding regions of *OsSPLs* and *OsSHR1* were cloned into the pB42AD vector; promoter regions of *OsSHR1* and *OsSWEETs* were cloned into the pLacZi reporter vector. Various combinations of plasmids were then co-transformed into the yeast (*S. cerevisiae*) strain EGY48, with combinations with empty pB42AD used as negative controls. Transformants were grown on SD/−Trp/−Ura agar medium at 30°C until colonies appeared. Colonies were then plated onto X-gal (5-bromo-4-chloro-3-indolyl-β-d-galactopyranoside) agar medium for blue colour development. Primers used for this assay are listed in Table S1.

4.5 | Y2H Assay

Full-length coding regions of *D53* and *OsSPL3/12/14* were cloned into pGBKT7 and pGADT7, respectively, to form BD-D53 and AD-OsSPL3/12/14. Various combinations of plasmids were then co-transformed into the yeast strain AH109; the combination of BD-D53 and AD-OsDLT2 was used as a negative control. Transformants were grown on SD/−Leu/−Trp agar medium at 30°C until colonies appeared. Colonies were then plated onto SD/−Ade/−His/−Leu/−Trp dropout screen medium to test protein interactions. Primers used for this assay are listed in Table S1.

4.6 | Expression and Purification of Fusion Proteins

The full-length CDS of *OsSPL3/12/14* and *OsSHR1* was cloned into the pGEX4T-1 vector, generating a fusion with the GST protein. The constructs of OsSPL3/12/14-GST, OsSHR1-GST and empty GST vectors were transformed into *Escherichia coli* BL21 (DE3) to induce protein expression. GST and GST labelled proteins were eluted with 50 mM glutathione. Primers used for this assay are listed in Table S1.

4.7 | Electrophoretic Mobility Shift Assay

The EMSA assay was performed using the LightShift Chemiluminescent EMSA kit (Thermo Fisher Scientific, 20148), according to the manufacturer's instructions. Oligonucleotide probes were synthesised and labelled with biotin by Thermo Fisher Scientific. The probe sequences are listed in Table S3.

4.8 | LUC Activity Determination

Promoter regions of *OsSHR1* and *OsSWEET2a/4/16* were cloned into the vector pGreenII0800-LUC to generate the ProOsSHR1:LUC and ProOsSWEET2a/4/16:LUC reporters. Full-length coding regions of *D53* and *OsSHR1* were cloned into the pAN580-GFP vector to generate the Pro35S:D53-GFP and Pro35S:OsSHR1-GFP effectors. Full-length coding regions of *OsSPL3/12/14* were cloned into the vector pCAMBIA1300-Flag to generate the Pro35S:OsSPL3/12/14-Flag effectors. The combined reporter and effector plasmids were then co-transformed into rice protoplasts; combinations with empty vectors were used as negative controls. The *LUC* gene from *Renilla reniformis (Ren)* under the control of the CaMV35S promoter was used as an internal control. The LUC activities were determined by the Dual-luciferase Assay Kit (Promega, E1910) following the manufacturer's recommendations, and the relative LUC activity was calculated as the ratio of LUC/REN. Primers used for this assay are listed in Table S1.

4.9 | ChIP-qPCR Assay

Rice protoplasts co-transfected with Pro35S:OsSPL3/12/14-Flag and ProOsSHR1:LUC vectors were used to test the enrichment of OsSPL3/12/14 on the promoter regions of *OsSHR1*. The Flag antibodies were used for detection (Figure 2a–d). Rice protoplasts co-transfected with Pro35S:OsSHR1-GFP and ProOsSWEET2a/4/16:LUC vectors were used to test the enrichment of OsSHR1 on the promoter regions of *OsSWEET2a/4/16*. The GFP antibodies were used for detection (Figure 2g–j). No addition of antibodies (No Ab) served as negative controls.

Detailed procedures for ChIP assays were performed according to the previously reported method (Duan et al. 2019). Primers used for this assay are listed in Tables S1 and S2.

4.10 | Luciferase Complementation Imaging Assay

Full-length coding regions of *D53* and *OsSPL3/12/14* were cloned into the pCAMBIA1300-nLUC and pCAMBIA1300-cLUC vectors, respectively. These vectors were introduced into *A. tumefaciens* strain EHA105, and various combinations of EHA105 strains were co-infiltrated into *N. benthamiana* leaves. The combination of pCAMBIA1300-D53-nLUC and pCAMBIA1300-OsDLT2-cLUC was used as a negative control. After 36 to 48 h, leaves were treated with 1 mM luciferin (E1601, Promega) for 5 min, and luciferase activities were measured using an imaging apparatus (NightShade LB 985, Berthold). Primers used for this assay are listed in Table S1.

4.11 | Bimolecular Fluorescence Complementation Assays

Full-length coding regions of *OsSPL3/12/14* were ligated into the C-terminal fragment of yellow fluorescent protein (YFP) in p2YC vector to generate the Y^C-OsSPL3/12/14 constructs, and the full-length coding region of *D53* was ligated into the N-terminal fragment of YFP in p2YN vector to generate the Y^N-D53 construct. These constructs were introduced into *A. tumefaciens* strain EHA105, and various combinations of EHA105 strains were co-infiltrated into *N. benthamiana* leaves. The combination of Y^N-D53 and Y^C-OsDLT2 was used as a negative control. After 36 to 48 h, leaves were harvested for fluorescence signal capture using a laser scanning confocal microscope (ZEISS LSM 980). Primers used for this assay are listed in Table S1.

4.12 | Antibody Preparation and Immunoblot Analyses

The antibody against OsSHR1 was previously described (Lin et al. 2020). For the detection of OsSWEET16, a SUMO-fused protein-specific polypeptide (amino acids 216–328 of OsSWEET16 protein) was expressed in *E.coli* Rosetta cells, and then affinity purified. Subsequently, the recombination protein was injected into rabbits to produce polyclonal antibodies against OsSWEET16 at ABclonal Technology. Fractionation of proteins and the immunoblotting assay were performed as previously described (Duan et al. 2023), and immunoblotted with anti-OsSHR1 antibody (1:2000), anti-OsSWEET16 antibody (1:2000) and anti-HSP82 antibody (AbM51099-31-PU, Beijing Protein Innovation, 1:5000).

4.13 | Co-Immunoprecipitation Assay

Full-length coding regions of *D53* and *OsSPL3/12/14* were ligated into the pCAMBIA1305-GFP and pCAMBIA1300-Flag vectors to produce the Pro35S:D53-GFP and Pro35S:OsSPL3/12/14-Flag constructs, respectively. The constructs were introduced into *A. tumefaciens* strain EHA105, and then co-infiltrated into *N. benthamiana* leaves. After 36 h treatment, total protein was extracted from infiltrated *N. benthamiana* leaves. Immunoblots were analysed with anti-Flag antibody (M185-7, MBL, 1:5000) and anti-GFP antibody (11 814 460 001, Roche, 1:5000). Primers used for this assay are listed in Table S1.

4.14 | GR24 and Sugar Treatment

Germinated seeds were sown on floating nets and grown in hydroponic culture with $GR24^{5DS}$ (1 μM) or sugar (0.5%, 1% and 2% w/v). Then the root lengths and crown root numbers were measured after treatment. Samples were harvested at indicated time points. RNA isolation, cDNA synthesis, RT-qPCR, protein extraction and immunoblotting were performed as described above.

4.15 | Subcellular Localization Analysis

Subcellular localization of OsSWEET2a/4/16 was detected using the cDNA (without stop codons) sequence of *OsSWEET2a/4/16* fused in-frame into the pAN580-GFP vector driven by the 35S promoter. Rice protoplasts were isolated from Nip stem base. A total of 10 μg plasmids (pOsSWEET2a/4/16-GFP and OsSCAMP1-mCherry or OsVIT1-mCherry) were transformed into rice protoplasts by the polyethylene-glycol-mediated method. After incubation in the dark for 12 ~ 15 h at 28°C, a confocal laser scanning microscope (STELLARIS 5, Leica; Germany) was used to observe the fluorescence signals in transformed protoplasts. The OsSCAMP1-mCherry and OsVIT1-mCherry were selected as the plasma membrane and tonoplast localization markers, respectively.

4.16 | Complementation Assays for OsSWEET2a/4/16 in Yeast

For complementation assays in yeast cells, the ORFs of the three *OsSWEETs* with XhoI were cloned into the yeast expression vector pDR196. Subsequently, the resulting constructs were transformed into the hexose transport-deficient yeast strain EBY.VW4000 and the sucrose uptake-deficient yeast strain SUSY7/ura3. Transformants of the hexose transport-deficient strain were grown on liquid SD/−uracil media supplemented with 2% maltose (glucose was used for the sucrose uptake-deficient strain). Serial dilutions of yeast cell suspensions of EBY.VW4000 were added dropwise onto solid SD/uracil media consisting of either 2% maltose or 2% glucose/fructose. Similarly, serial dilutions of yeast cell suspensions of SUSY7/ura3 were added dropwise onto solid SD/−uracil media consisting of 2% glucose or 2% sucrose. Growth was documented via imaging after 3 to 4 days of growth at 30°C.

4.17 | Glucose, Fructose and Sucrose Measurements

At the end of the dark, samples were collected from the rice seedlings of Nip, *OsSHR1-Ri* and *ossweet2a/4/16* mutants with or without $GR24^{5DS}$ treatment. All samples were frozen and ground into powder, and then 0.1 g of the fresh sample was

weighed and placed into a 2 mL tube. Subsequently, 1 mL of 50% ethanol was added to each tube, and the mixture was sonicated for 30 min. The samples were centrifuged at 11 500 *g* for 5 min, and the supernatant was aspirated. The soluble sugar content was determined by using high performance liquid chromatography (UHPLC3600, Wayeal, China). The standard curve was prepared with glucose, fructose and sucrose standards.

4.18 | Starch Iodine Staining

The stem bases were soaked in 100% (v/v) ethanol to remove chlorophyll, then rinsed in water to remove excess ethanol (root tips do not need this treatment). This was followed by staining in Lugol solution (Sigma) for 10 min as previously reported (Seung et al. 2015). The samples were then destained in water for several hours for optimal visualisation.

4.19 | RNA In Situ Hybridization

RNA in situ hybridization was performed as previously described (Lin et al. 2012). Shoot bases of rice seedlings at the third and fourth leaf stages were fixed in cold, freshly prepared FAA overnight at 4°C, then dehydrated, clarified and embedded in paraffin (Paraplast Plus; Sigma-Aldrich) in sequence. Thin sections of paraffin-embedded shoot bases of 8 to 12 μm thickness were generated for the hybridization. Specific encoding fragments of *OsSHR1* and *OsSWEET2a/4/16* were selected for synthesis of digoxigenin (DIG)-labelled RNA sense and antisense probes in vitro by DIG RNA Labeling Kit (Roche). The hybridization reaction was conducted for 16 h at 50°C. Anti-DIG alkaline phosphatase-conjugated antibody and the NBT/BCIP staining method were used to visualise the tissue-specific localization of gene expression in shoot base sections.

4.20 | Statistical Analysis

The data were collected by Microsoft Excel. All collected data were analysed using GraphPad Prism 8. Two-tailed Student's *t*-test, one-way ANOVA or two-way ANOVA tests were performed to test the statistical significance. p value < 0.05 was considered statistically significant. Graphs were plotted by GraphPad Prism 8 and edited by Adobe Illustrator.

4.21 | Accession Numbers

Genome sequence data from this study can be found in the EMBL/GenBank data libraries under the following accession numbers: *OsSHR1*, Os07g0586900; *D53*, Os11g0104300; *OsSPL3*, Os02g0139400; *OsSPL12*, Os06g0703500; *OsSPL14*, Os08g0509600; *OsSWEET2a*, Os01g0541800; *OsSWEET4*, Os02g0301100; *OsSWEET16*, Os03g0341300.

Author Contributions

Jianmin Wan and Qibing Lin supervised the project. Miao Feng and Qibing Lin designed the research and wrote the paper. Miao Feng, Wenfan Luo, Sheng Luo, Rong Miao performed the experiments. Manpo Gu, Shuai Li, Xinxin Xing, Jinhui Zhang, Jinsheng Qian, Xin Liu, Chunlei Zhou, Qi Sun, Tong Luo, Nuo Chen, Yulong Ren, Zhijun Cheng, Cailin Lei, Zhichao Zhao, Shanshan Zhu, Xin Wang, Xiuping Guo provided technical assistance. All authors read and approved the final article.

Acknowledgements

This research was supported by grants from the National Key Research and Development Program of China (2022YFD1200104) and the Innovation Program of Chinese Academy of Agricultural Sciences (CAAS-CSCB-202401), the Central Public-interest Scientific Institution Basal Research Fund (No. Y2024YJ13) and the National Natural Science Foundation of China (31671769).

Conflicts of Interest

The authors declare no conflicts of interest.

Data Availability Statement

The data that support the findings of this study are available on request from the corresponding author. The data are not publicly available due to privacy or ethical restrictions.

References

Arite, T., H. Kameoka, and J. Kyozuka. 2011. "Strigolactone Positively Controls Crown Root Elongation in Rice." *Journal of Plant Growth Regulation* 31: 165–172.

Arite, T., M. Umehara, S. Ishikawa, et al. 2009. "*d14*, a Strigolactone-Insensitive Mutant of Rice, Shows an Accelerated Outgrowth of Tillers." *Plant and Cell Physiology* 50: 1416–1424.

Benfey, P. N., P. J. Linstead, K. Roberts, J. W. Schiefelbein, M.-T. Hauser, and R. A. Aeschbacher. 1993. "Root Development in Arabidopsis: Four Mutants With Dramatically Altered Root Morphogenesis." *Development* 119: 57–70.

Bertheloot, J., F. Barbier, F. Boudon, et al. 2019. "Sugar Availability Suppresses the Auxin-Induced Strigolactone Pathway to Promote Bud Outgrowth." *New Phytologist* 225: 866–879.

Birkenbihl, R. P., G. Jach, H. Saedler, and P. Huijser. 2005. "Functional Dissection of the Plant-Specific SBP-Domain: Overlap of the DNA-Binding and Nuclear Localization Domains." *Journal of Molecular Biology* 352: 585–596.

Breia, R., A. Conde, H. Badim, A. M. Fortes, H. Gerós, and A. Granell. 2021. "Plant SWEETs: From Sugar Transport to Plant–Pathogen Interaction and More Unexpected Physiological Roles." *Plant Physiology* 186: 836–852.

Chardon, F., M. Bedu, F. Calenge, et al. 2013. "Leaf Fructose Content Is Controlled by the Vacuolar Transporter SWEET17 in Arabidopsis." *Current Biology* 23: 697–702.

Chen, L., B. Hou, S. Lalonde, et al. 2010. "Sugar Transporters for Intercellular Exchange and Nutrition of Pathogens." *Nature* 468: 527–532.

Chen, L., X. Qu, B. Hou, et al. 2012. "Sucrose Efflux Mediated by SWEET Proteins as a Key Step for Phloem Transport." *Science* 335: 207–211.

Choi, J. W., and J. Lim. 2016. "Control of Asymmetric Cell Divisions During Root Ground Tissue Maturation." *Molecules and Cells* 39: 524–529.

Chu, Z., M. Yuan, J. Yao, et al. 2006. "Promoter Mutations of an Essential Gene for Pollen Development Result in Disease Resistance in Rice." *Genes & Development* 20: 1250–1255.

Cui, H., D. Kong, X. Liu, and Y. Hao. 2014. "*SCARECROW*, *SCR-LIKE 23* and *SHORT-ROOT* Control Bundle Sheath Cell Fate and Function in *Arabidopsis thaliana*." *Plant Journal* 78: 319–327.

de Saint Germain, A., G. Clavé, M.-A. Badet-Denisot, et al. 2016. "An Histidine Covalent Receptor and Butenolide Complex Mediates Strigolactone Perception." *Nature Chemical Biology* 12: 787–794.

Dhondt, S., F. Coppens, F. De Winter, et al. 2010. "*SHORT-ROOT* and *SCARECROW* Regulate Leaf Growth in Arabidopsis by Stimulating S-Phase Progression of the Cell Cycle." *Plant Physiology* 154: 1183–1195.

Di Laurenzio, L., J. Wysocka Diller, J. E. Malamy, et al. 1996. "The *SCARECROW* Gene Regulates an Asymmetric Cell Division That Is Essential for Generating the Radial Organization of the Arabidopsis Root." *Cell* 86: 423–433.

Dong, W., Y. Zhu, H. Chang, et al. 2020. "An SHR–SCR Module Specifies Legume Cortical Cell Fate to Enable Nodulation." *Nature* 589: 586–590.

Duan, E., Q. Lin, Y. Wang, et al. 2023. "The Transcriptional Hub SHORT INTERNODES1 Integrates Hormone Signals to Orchestrate Rice Growth and Development." *Plant Cell* 35: 2871–2886.

Duan, E., Y. Wang, X. Li, et al. 2019. "OsSHI1 Regulates Plant Architecture Through Modulating the Transcriptional Activity of IPA1 in Rice." *Plant Cell* 31: 1026–1042.

Fukaki, H., J. Wysocka-Diller, T. Kato, H. Fujisawa, P. N. Benfey, and M. Tasaka. 1998. "Genetic Evidence That the Endodermis Is Essential for Shoot Gravitropism in *Arabidopsis thaliana*." *Plant Journal* 14: 425–430.

Gao, Y., C. Y. Xue, J. M. Liu, et al. 2021. "Sheath Blight Resistance in Rice Is Negatively Regulated by WRKY53 via *SWEET2a* Activation." *Biochemical and Biophysical Research Communications* 585: 117–123.

Gao, Y., C. Zhang, X. Han, et al. 2018. "Inhibition of *OsSWEET11* Function in Mesophyll Cells Improves Resistance of Rice to Sheath Blight Disease." *Molecular Plant Pathology* 19: 2149–2161.

Gao, Z., Q. Qian, X. Liu, et al. 2009. "*Dwarf 88*, a Novel Putative Esterase Gene Affecting Architecture of Rice Plant." *Plant Molecular Biology* 71: 265–276.

Gomez-Roldan, V., S. Fermas, P. B. Brewer, et al. 2008. "Strigolactone Inhibition of Shoot Branching." *Nature* 455: 189–194.

Gong, X., M. A. Flores-Vergara, J. H. Hong, et al. 2016. "*SEUSS* Integrates Gibberellin Signaling With Transcriptional Inputs From the SHR-SCR-SCL3 Module to Regulate Middle Cortex Formation in the Arabidopsis Root." *Plant Physiology* 170: 1675–1683.

Guo, W., R. Nagy, H. Chen, et al. 2014. "SWEET17, a Facilitative Transporter, Mediates Fructose Transport Across the Tonoplast of Arabidopsis Roots and Leaves." *Plant Physiology* 164: 777–789.

Helariutta, Y., H. Fukaki, J. Wysoka-Diller, et al. 2000. "The *SHORT-ROOT* Gene Controls Radial Patterning of the Arabidopsis Root Through Radial Signaling." *Cell* 101: 555–567.

Henry, S., A. Dievart, F. Divol, et al. 2017. "*SHR* Overexpression Induces the Formation of Supernumerary Cell Layers With Cortex Cell Identity in Rice." *Developmental Biology* 425: 1–7.

Hirsch, S., J. Kim, A. Muñoz, A. B. Heckmann, J. A. Downie, and G. E. D. Oldroyd. 2009. "GRAS Proteins Form a DNA Binding Complex to Induce Gene Expression During Nodulation Signaling in *Medicago truncatula*." *Plant Cell* 21: 545–557.

Hu, Q., H. Liu, Y. He, et al. 2024. "Regulatory Mechanisms of Strigolactone Perception in Rice." *Cell* 187: 7551–7567.

Hu, Z., Z. Tang, Y. Zhang, et al. 2021. "Rice SUT and SWEET Transporters." *International Journal of Molecular Sciences* 22: 11198.

Inukai, Y., T. Sakamoto, M. Ueguchi-Tanaka, et al. 2005. "*Crown rootless1*, Which Is Essential for Crown Root Formation in Rice, Is a Target of an AUXIN RESPONSE FACTOR in Auxin Signaling." *Plant Cell* 17: 1387–1396.

Ishikawa, S., M. Maekawa, T. Arite, K. Onishi, I. Takamure, and J. Kyozuka. 2005. "Suppression of Tiller Bud Activity in Tillering Dwarf Mutants of Rice." *Plant and Cell Physiology* 46: 79–86.

Jeena, G. S., S. Kumar, and R. K. Shukla. 2019. "Structure, Evolution and Diverse Physiological Roles of SWEET Sugar Transporters in Plants." *Plant Molecular Biology* 100: 351–365.

Jiang, L., X. Liu, G. Xiong, et al. 2013. "*DWARF 53* Acts as a Repressor of Strigolactone Signalling in Rice." *Nature* 504: 401–405.

Jiao, Y., Y. Wang, D. Xue, et al. 2010. "Regulation of *OsSPL14* by OsmiR156 Defines Ideal Plant Architecture in Rice." *Nature Genetics* 42: 541–544.

Kapulnik, Y., P.-M. Delaux, N. Resnick, et al. 2011. "Strigolactones Affect Lateral Root Formation and Root-Hair Elongation in Arabidopsis." *Planta* 233: 209–216.

Kerr, S. C., and C. A. Beveridge. 2017. "IPA1: A Direct Target of SL Signaling." *Cell Research* 27: 1191–1192.

Kim, P., C. Y. Xue, H. D. Song, et al. 2021. "Tissue-Specific Activation of *DOF11* Promotes Rice Resistance to Sheath Blight Disease and Increases Grain Weight via Activation of *SWEET14*." *Plant Biotechnology Journal* 19: 409–411.

Klemens, P. A. W., K. Patzke, J. Deitmer, et al. 2013. "Overexpression of the Vacuolar Sugar Carrier AtSWEET16 Modifies Germination, Growth, and Stress Tolerance in Arabidopsis." *Plant Physiology* 163: 1338–1352.

Koltai, H. 2011. "Strigolactones Are Regulators of Root Development." *New Phytologist* 190: 545–549.

Kumar, M., N. Pandya-Kumar, Y. Kapulnik, and H. Koltai. 2015. "Strigolactone Signaling in Root Development and Phosphate Starvation." *Plant Signaling & Behavior* 10: e1045174.

Lee, J., J.-J. Park, S. L. Kim, J. Yim, and G. An. 2007. "Mutations in the Rice Liguleless Gene Result in a Complete Loss of the Auricle, Ligule, and Laminar Joint." *Plant Molecular Biology* 65: 487–499.

Lee, S. A., S. Jang, E. K. Yoon, et al. 2016. "Interplay Between ABA and GA Modulates the Timing of Asymmetric Cell Divisions in the Arabidopsis Root Ground Tissue." *Molecular Plant* 9: 870–884.

Li, X., Q. Qian, Z. Fu, et al. 2003. "Control of Tillering in Rice." *Nature* 422: 618–621.

Liao, Z., H. Yu, J. Duan, et al. 2019. "SLR1 Inhibits MOC1 Degradation to Coordinate Tiller Number and Plant Height in Rice." *Nature Communications* 10: 2738.

Lin, I. W., D. Sosso, L.-Q. Chen, et al. 2014. "Nectar Secretion Requires Sucrose Phosphate Synthases and the Sugar Transporter SWEET9." *Nature* 508: 546–549.

Lin, Q., D. Wang, H. Dong, et al. 2012. "Rice APC/C^{TE} Controls Tillering by Mediating the Degradation of MONOCULM 1." *Nature Communications* 3: 752.

Lin, Q., Z. Zhang, F. Wu, et al. 2020. "The APC/C^{TE} E3 Ubiquitin Ligase Complex Mediates the Antagonistic Regulation of Root Growth and Tillering by ABA and GA." *Plant Cell* 32: 1973–1987.

Liu, Q., S. Teng, C. Deng, et al. 2023. "SHORT ROOT and INDETERMINATE DOMAIN Family Members Govern *PIN-FORMED* Expression to Regulate Minor Vein Differentiation in Rice." *Plant Cell* 35: 2848–2870.

Lu, Z., H. Yu, G. Xiong, et al. 2013. "Genome-Wide Binding Analysis of the Transcription Activator IDEAL PLANT ARCHITECTURE1

Reveals a Complex Network Regulating Rice Plant Architecture." *Plant Cell* 25: 3743–3759.

Ma, L., D. Zhang, Q. Miao, J. Yang, Y. Xuan, and Y. Hu. 2017. "Essential Role of Sugar Transporter OsSWEET11 During the Early Stage of Rice Grain Filling." *Plant and Cell Physiology* 58: 863–873.

Mathan, J., A. Singh, and A. Ranjan. 2021. "Sucrose Transport in Response to Drought and Salt Stress Involves ABA-Mediated Induction of *OsSWEET13* and *OsSWEET15* in Rice." *Physiologia Plantarum* 171: 620–637.

Miura, K., M. Ikeda, A. Matsubara, et al. 2010. "*OsSPL14* Promotes Panicle Branching and Higher Grain Productivity in Rice." *Nature Genetics* 42: 545–549.

Morii, M., A. Sugihara, S. Takehara, et al. 2020. "The Dual Function of OsSWEET3a as a Gibberellin and Glucose Transporter Is Important for Young Shoot Development in Rice." *Plant and Cell Physiology* 61: 1935–1945.

Nakajima, K., G. Sena, T. Nawy, and P. N. Benfey. 2001. "Intercellular Movement of the Putative Transcription Factor *SHR* in Root Patterning." *Nature* 413: 307–311.

Ortiz-Ramírez, C., B. Guillotin, X. Xu, et al. 2021. "Ground Tissue Circuitry Regulates Organ Complexity in Maize and *Setaria*." *Science* 374: 1247–1252.

Patil, S. B., F. F. Barbier, J. Zhao, et al. 2021. "Sucrose Promotes D53 Accumulation and Tillering in Rice." *New Phytologist* 234: 122–136.

Quirino, B. F., J. Normanly, and R. M. Amasino. 1999. "Diverse Range of Gene Activity During *Arabidopsis thaliana* Leaf Senescence Includes Pathogen-Independent Induction of Defense-Related Genes." *Plant Molecular Biology* 40: 267–278.

Rasmussen, A., M. G. Mason, C. De Cuyper, et al. 2012. "Strigolactones Suppress Adventitious Rooting in Arabidopsis and Pea." *Plant Physiology* 158: 1976–1987.

Ruyter-Spira, C., W. Kohlen, T. Charnikhova, et al. 2011. "Physiological Effects of the Synthetic Strigolactone Analog GR24 on Root System Architecture in Arabidopsis: Another Belowground Role for Strigolactones?" *Plant Physiology* 155: 721–734.

Schleucher, J., P. J. Vanderveer, and T. D. Sharkey. 1998. "Export of Carbon From Chloroplasts at Night." *Plant Physiology* 118: 1439–1445.

Schuler, M. L., O. V. Sedelnikova, B. J. Walker, P. Westhoff, and J. A. Langdale. 2018. "SHORTROOT-Mediated Increase in Stomatal Density Has no Impact on Photosynthetic Efficiency." *Plant Physiology* 176: 757–772.

Seung, D., S. Soyk, M. Coiro, B. A. Maier, S. Eicke, and S. C. Zeeman. 2015. "PROTEIN TARGETING TO STARCH Is Required for Localising GRANULE-BOUND STARCH SYNTHASE to Starch Granules and for Normal Amylose Synthesis in Arabidopsis." *PLoS Biology* 13: e1002080.

Shabek, N., F. Ticchiarelli, H. Mao, T. R. Hinds, O. Leyser, and N. Zheng. 2018. "Structural Plasticity of D3–D14 Ubiquitin Ligase in Strigolactone Signalling." *Nature* 563: 652–656.

Shao, G., Z. Lu, J. Xiong, et al. 2019. "Tiller Bud Formation Regulators MOC1 and MOC3 Cooperatively Promote Tiller Bud Outgrowth by Activating FON1 Expression in Rice." *Molecular Plant* 12: 1090–1102.

Shao, Y., H. Zhou, Y. Wu, et al. 2019. "*OsSPL3*, an SBP-Domain Protein, Regulates Crown Root Development in Rice." *Plant Cell* 31: 1257–1275.

Shi, C., P. Luo, Y. Du, et al. 2019. "Maternal Control of Suspensor Programmed Cell Death via Gibberellin Signaling." *Nature Communications* 10: 3484.

Si, L., J. Chen, X. Huang, et al. 2016. "*OsSPL13* Controls Grain Size in Cultivated Rice." *Nature Genetics* 48: 447–456.

Singh, J., S. Das, K. Jagadis Gupta, A. Ranjan, C. H. Foyer, and J. K. Thakur. 2023. "Physiological Implications of SWEETs in Plants and Their Potential Applications in Improving Source–Sink Relationships for Enhanced Yield." *Plant Biotechnology Journal* 21: 1528–1541.

Snowden, K. C., A. J. Simkin, B. J. Janssen, et al. 2005. "The Decreased Apical dominance1/*Petunia hybrida* CAROTENOID CLEAVAGE DIOXYGENASE8 Gene Affects Branch Production and Plays a Role in Leaf Senescence, Root Growth, and Flower Development." *Plant Cell* 17: 746–759.

Song, X., Z. Lu, H. Yu, et al. 2017. "IPA1 Functions as a Downstream Transcription Factor Repressed by D53 in Strigolactone Signaling in Rice." *Cell Research* 27: 1128–1141.

Sosso, D., D. Luo, Q.-B. Li, et al. 2015. "Seed Filling in Domesticated Maize and Rice Depends on SWEET-Mediated Hexose Transport." *Nature Genetics* 47: 1489–1493.

Sun, H., X. Guo, X. Qi, et al. 2021. "SPL14/17 Act Downstream of Strigolactone Signalling to Modulate Rice Root Elongation in Response to Nitrate Supply." *Plant Journal* 106: 649–660.

Sun, H., J. Tao, P. Gu, G. Xu, and Y. Zhang. 2016. "The Role of Strigolactones in Root Development." *Plant Signaling & Behavior* 11: e1110662.

Sun, H., J. Tao, S. Liu, et al. 2014. "Strigolactones Are Involved in Phosphate- and Nitrate-Deficiency-Induced Root Development and Auxin Transport in Rice." *Journal of Experimental Botany* 65: 6735–6746.

Takahashi, I., K. Jiang, and T. Asami. 2021. "Counteractive Effects of Sugar and Strigolactone on Leaf Senescence of Rice in Darkness." *Agronomy* 11: 1044.

Tian, M., K. Jiang, I. Takahashi, and G. Li. 2018. "Strigolactone-Induced Senescence of a Bamboo Leaf in the Dark Is Alleviated by Exogenous Sugar." *Journal of Pesticide Science* 43: 173–179.

Tong, H., Y. Jin, W. Liu, et al. 2009. "DWARF AND LOW-TILLERING, a New Member of the GRAS Family, Plays Positive Roles in Brassinosteroid Signaling in Rice." *Plant Journal* 58: 803–816.

Tong, H., L. Liu, Y. Jin, et al. 2012. "DWARF AND LOW-TILLERING Acts as a Direct Downstream Target of a GSK3/SHAGGY-Like Kinase to Mediate Brassinosteroid Responses in Rice." *Plant Cell* 24: 2562–2577.

Ueda, H., and M. Kusaba. 2015. "Strigolactone Regulates Leaf Senescence in Concert With Ethylene in Arabidopsis." *Plant Physiology* 169: 138–147.

Umehara, M., A. Hanada, S. Yoshida, et al. 2008. "Inhibition of Shoot Branching by New Terpenoid Plant Hormones." *Nature* 455: 195–200.

Valifard, M., R. Le Hir, J. Müller, D. Scheuring, H. E. Neuhaus, and B. Pommerrenig. 2021. "Vacuolar Fructose Transporter SWEET17 Is Critical for Root Development and Drought Tolerance." *Plant Physiology* 187: 2716–2730.

Wang, P., S. Kelly, J. P. Fouracre, and J. A. Langdale. 2013. "Genome-Wide Transcript Analysis of Early Maize Leaf Development Reveals Gene Cohorts Associated With the Differentiation of C4 Kranz Anatomy." *Plant Journal* 75: 656–670.

Wang, Q., A. Sun, S. Chen, L. Chen, and F. Guo. 2018. "*SPL6* Represses Signalling Outputs of ER Stress in Control of Panicle Cell Death in Rice." *Nature Plants* 4: 280–288.

Wang, S., K. Wu, Q. Yuan, et al. 2012. "Control of Grain Size, Shape and Quality by *OsSPL16* in Rice." *Nature Genetics* 44: 950–954.

Wu, L. B., J. S. Eom, R. Isoda, et al. 2022. "*OsSWEET11b*, a Potential Sixth Leaf Blight Susceptibility Gene Involved in Sugar Transport-Dependent Male Fertility." *New Phytologist* 234: 975–989.

Wu, Z., L. Chen, Q. Yu, et al. 2019. "Multiple Transcriptional Factors Control Stomata Development in Rice." *New Phytologist* 223: 220–232.

Xie, K., C. Wu, and L. Xiong. 2006. "Genomic Organization, Differential Expression, and Interaction of SQUAMOSA Promoter-Binding-Like Transcription Factors and microRNA156 in Rice." *Plant Physiology* 142: 280–293.

Yamasaki, K., T. Kigawa, M. Inoue, et al. 2004. "A Novel Zinc-Binding Motif Revealed by Solution Structures of DNA-Binding Domains of Arabidopsis SBP-Family Transcription Factors." *Journal of Molecular Biology* 337: 49–63.

Yang, B., A. Sugio, and F. F. White. 2006. "*Os8N3* Is a Host Disease-Susceptibility Gene for Bacterial Blight of Rice." *Proceedings of the National Academy of Sciences* 103: 10503–10508.

Yang, J., D. Luo, B. Yang, W. B. Frommer, and J. S. Eom. 2018. "*SWEET11* and *15* as Key Players in Seed Filling in Rice." *New Phytologist* 218: 604–615.

Yang, S., Y. Fu, Y. Zhang, et al. 2023. "Rhizoctonia Solani Transcriptional Activator Interacts With Rice WRKY53 and Grassy Tiller 1 to Activate SWEET Transporters for Nutrition." *Journal of Advanced Research* 50: 1–12.

Yao, R., Z. Ming, L. Yan, et al. 2016. "DWARF14 Is a Non-Canonical Hormone Receptor for Strigolactone." *Nature* 536: 469–473.

Yuan, K., H. Zhang, C. Yu, et al. 2023. "Low Phosphorus Promotes NSP1–NSP2 Heterodimerization to Enhance Strigolactone Biosynthesis and Regulate Shoot and Root Architecture in Rice." *Molecular Plant* 16: 1811–1831.

Yuan, M., and S. Wang. 2013. "Rice *MtN3/Saliva/SWEET* Family Genes and Their Homologs in Cellular Organisms." *Molecular Plant* 6: 665–674.

Yuan, M., J. Zhao, R. Huang, X. Li, J. Xiao, and S. Wang. 2014. "Rice *MtN3/Saliva/SWEET* Gene Family: Evolution, Expression Profiling, and Sugar Transport." *Journal of Integrative Plant Biology* 56: 559–570.

Zhang, L., H. Yu, B. Ma, et al. 2017. "A Natural Tandem Array Alleviates Epigenetic Repression of *IPA1* and Leads to Superior Yielding Rice." *Nature Communications* 8: 14789.

Zhong, Y., Y. Wang, X. Pan, et al. 2024. "*ZmCCD8* Regulates Sugar and Amino Acid Accumulation in Maize Kernels via Strigolactone Signalling." *Plant Biotechnology Journal* 23: 492–508.

Zhou, F., Q. Lin, L. Zhu, et al. 2013. "D14–SCF^{D3}-Dependent Degradation of D53 Regulates Strigolactone Signalling." *Nature* 504: 406–410.

Zhou, Y., L. Liu, W. Huang, et al. 2014. "Overexpression of *OsSWEET5* in Rice Causes Growth Retardation and Precocious Senescence." *PLoS One* 9: e94210.

Supporting Information

Additional supporting information can be found online in the Supporting Information section. **Figure S1:** The expression pattern of *OsSHR1* in seedlings and heading stage plants. **Figure S2:** OsSPL3/12/14 directly binds to the promoter of *OsSHR1*. **Figure S3:** OsSPL3/12/14 interacts with D53 in vivo and in vitro. **Figure S4:** OsSHR1 directly binds to the promoters of *OsSWEET2a/4/16* in yeast. **Figure S5:** OsSHR1 directly binds to the promoters of *OsSWEET2a/4/16* in EMSA. **Figure S6:** *OsSHR1* acts downstream of *OsSPL14* to regulate tillering. **Figure S7:** *OsSHR1* acts downstream of *OsSPL3* to regulate tillering. **Figure S8:** *OsSHR1* acts downstream of *OsSPL12* to regulate tillering. **Figure S9:** Root morphology of *OsSHR1--Ri*, *osspl14* and *OsSHR1-Ri/osspl14* plants. **Figure S10:** *OsSHR1* acts downstream of *OsSPL3* to regulate root development. **Figure S11:** *OsSHR1* acts downstream of *OsSPL12* to regulate root development. **Figure S12:** Reduced expression levels of *OsSHR1* in *OsSPL3/12* mutants. **Figure S13:** The relationship between *OsSHR1* and *OsSWEET2a* in regulating tillering. **Figure S14:** The relation between *OsSWEET4* and *OsSHR1*in regulating tillering. **Figure S15:** *OsSHR1* acts upstream of *OsSWEET2a* to regulate root development. **Figure S16:** The relation between *OsSWEET4* and *OsSHR1* in regulating root development. **Figure S17:** The expression of *OsSWEET16* in *OsSPL3/12/14* mutants. **Figure S18:** The expression of *OsSWEET2a/4* in *OsSHR1* and *OsSPL14* mutants. **Figure S19:** Subcellular localization of OsSWEET2a/4/16-GFP fusion proteins in rice protoplasts. **Figure S20:** Diurnal rhythmic expression of *OsSWEET16/2a/4* in tiller buds and roots under GR24^{5DS} treatment. **Figure S21:** Sugar treatments promote the growth of tiller buds. **Figure S22:** Sugar treatments regulate the root development of rice. **Figure S23:** Starch reacts with iodine to yield distinct colours that vary with its concentration. **Figure S24:** Expression pattern of *OsSWEET2a/4/16* in rice. **Table S1:** Primers used in this study for vector constructions. **Table S2:** Primers used for RT-qPCR and ChIP-qPCR analyses. **Table S3:** Oligonucleotides used for EMSA assays.